SYNTHESIS & CHARACTERIZATION OF “PLUM PUDDING” POLY (OLIGOETHYLENE GLYCOL METHYL METHACRYLATE) HYDROGELS USING STARCH NANOPARTICLES

By ALI AFFAR, H.B.SC.

A Thesis Submitted to the School of Graduate Studies in Partial Fulfillment of the Requirements for the Degree of Master of Applied Science

MASTER OF APPLIED SCIENCE (2019)

Department of Chemical Engineering

McMaster University

Hamilton, Ontario, Canada

TITLE: Synthesis & Characterization Of “Plum Pudding” Poly (Oligoethylene Glycol Methyl Methacrylate) Hydrogels Using Starch Nanoparticles

AUTHOR: Ali Affar, H.B.Sc. (McMaster University)

SUPERVISOR: Dr. Todd Hoare

NUMBER of PAGES: xii, 72, II

Abstract

Hydrogels are defined as swellable polymer networks with the mechanical, interfacial, and physical properties similar to native tissues in the body. Nanocomposite hydrogels, defined as hydrogels that either entirely consist of or have embedded nanoparticle phases, have been shown to further expand the range of properties achievable with hydrogels and be suitable in many applications such as building tissue scaffolds. In particular, nanocomposite phases that can be eroded offer interesting potential to construct nanoscale voids that can be made in the gel that may be highly beneficial for applications in drug delivery, bioseparations, and tissue engineering.

In this thesis, two methods of incorporating starch nanoparticles (SNPs) into a ultraviolet (UV)-cured poly(ethylene glycol methacrylate) (POEGMA) matrix are described. In the first method, the SNPs were physically entrapped during the curing of the gels. An investigation of the effect of fabrication parameters such as monomer ratios, crosslinker amounts, and entrapped SNP concentration on swelling and shear storage modulus (G') was performed. Enzymatic degradation of the nanophase was also observed to be possible upon amylase treatment, and the resulting internal morphology was confirmed to have increased internal porosity based on a methylene blue uptake experiment. In the second method, chemically functionalized SNPs were used as the exclusive crosslinker to create the POEGMA network. The swelling and mechanical performance of the SNP-crosslinked hydrogels were investigated and compared to the entrapped SNP gels. A preliminary study of the consequences of degradation of a naturally occurring crosslinker to the enzyme α-amylase was also performed. The combination of cytocompatible components and potential for internal porosity control make gels an interesting platform for tissue scaffolding and bioseparation applications.

Acknowledgements

I would firstly like to thank Dr. Todd Hoare for continued advice and support over the course of my time in his laboratory. To Michael Majcher and Dr. Niels Smeets, thank you for your ideas and contributions in the application of SNPs. Thank you for the support of EcoSynthetix Inc., namely Dennis Kinio and Dr. Steven Bloembergen, and the Department of Chemical Engineering for their administrative support over the course of this degree. This research project was funded by the National Science and Engineering Council of Canada through their Strategic Project Grants Program.

To my dear brothers in STEM Ali Babar, Ali (Matthew) Campea, Ali (Jonathan) Dorogin & Ali (Mitchell) Ross, thank you for being awesome friends and supportive colleagues over our time together in graduate school. Thank you for the talks, the daily lunches and coffee breaks where we discussed everything and nothing, creating memories along the way.

To my colleagues in the Hoare lab, namely Eva Mueller & Madeline Simpson, thank you for creating and sustaining an effective environment of cohesive interdisciplinary learning and research. To my dear post-doctoral fellow Xiaoyun Li, thank you so much for your guidance over our short time together. I wish you the best of luck with your research and future endeavors!

To my parents Samar Morsi & Nader Affar, I hope I have been able to make you proud and made all your sacrifices and unwavering support justified. To my sister Nadine, I hope my experience and ability to complete this degree motivates you and proves to you anything is possible if you apply yourself.

Last but certainly never least, thank you to my girlfriend Sejal Mistry for her constant support and unconditional love over these past 2 years of this degree, over the 10 years we have known each other and forever.

Table of Contents

List of Schemes and Figures

List of Abbreviations and Symbols

°C	Degrees Celsius
^{1}H NMR	Proton Nuclear Magnetic Resonance
3D	3 Dimensional
3T3	NIH mouse fibroblast line
BSA	Bovine serum albyumin
D_2O	Deuterated water
Da	Dalton (g/mol)
DMSO	Dimethyl Sulfoxide
ECM	Extracellular matrix
EDC	1-Ethyl-3-(3-dimethylaminopropyl)carbodiimide
FITC	Fluorescein isothiocyanate
G’	Shear storage modulus
HCl	Hydrochloric acid
kPa	kilopascal
LCST	Lower critical solution temperature
$M(EO)_2MA$	Diethylene glycol methacrylate
MEHQ	Methyl ether hydroquinone
MHz	Megahertz
MW	Molecular weight
MWCO	Molecular weight cut-off
NaOH	Sodium hydroxide
nm	Nanometers
OEGMA	Oligoethylene glycol methacrylate
PBS	Phosphate buffered saline
PEG	Poly(ethylene glycol)

SNP	Starch nanoparticle
TEMPO	2,2,6,6-Tetramethylpiperidin-1-yl)oxyl
UV	Ultraviolet

Declaration of Academic Achievement

The work described here in was conceived, conducted, analyzed and interpreted solely by the author of this work, with the following exception:

- Chapter 3: the experimental runs and interpretation of the results for the MicroSquisher compressive force testing was done in collaboration with Eva Mueller, the lab's MicroSquishing expert.

1 Introduction and Literature Review

1.1 – Hydrogels

Hydrogels are hydrophilic polymer networks which can imbibe water. The main difference between hydrogels and other analogous polymer structures is their ability to swell and resist total dissolution. This is due to network crosslinking, which allows the matrix to respond to its surroundings while maintaining its overall form.[1] There are many strategies for establishing these crosslinks, including covalent strategies (i.e. mixing polymers functionalized with complementary chemically reactive groups or using a small molecule bifunctional crosslinker) and physical strategies such as host-guest interactions or ionic/electrostatic interactions.[2] The most widely used approach for hydrogel fabrication is free radical chemistry, in which water soluble monomers are polymerized in the presence of a water-soluble crosslinker to form a network over three stages: 1) initiation of the radical species, 2) propagation of that radical species to other monomers, building a polymer chain, and 3) radical termination. Initiation is typically achieved using a free radical initiator that can be cleaved to form radicals either by heating (e.g. ammonium persulfate) or light (e.g. ultraviolet-induced cleavage of Irgacure 2959, or 2-hydroxy-4′-(2-hydroxyethoxy)-2-methylpropiophenone); in the latter case, irradiation with 365 nm light induces benzoyl radical oxidation by which the bond alpha to the carbonyl dissociates to create benzoyl and alkyl radicals.[3, 4]

Many parameters affect the final gel properties achieved. For example, the overall swelling and hydrophilicity of a hydrogel can be adjusted based on the chemistry and concentrations of the comonomers used, allowing for tuning of the swelling activity by modifying the overall hydrophilicity or crosslink density.[5] In particular, the use of certain gel building blocks can elicit macroscopic “smart” properties on the hydrogel when an external stimulus is applied. For example, cleavable functional groups can be incorporated into the crosslinker to facilitate gel degradation upon a change of pH,[1] a change in redox conditions (e.g. disulfide-linked crosslinks),[2] and/or the presence of enzymes such as amylase, lipase or esterase to act on sugars, lipids, and esters respectively.[6-9]

Alternatively, the use of monomers that can form polymers with lower critical solution temperatures (LCSTs) in water, such as N-isopropylacrylamide or oligoethylene glycol methacrylate, enable the formation of gels that can swell and shrink upon changes in temperature.[8, 10-12]

1.2 – Hydrogel Morphologies

The macroscopic properties of hydrogels are predominately dictated by the microscopic and molecular structure of the hydrogel. Many structures have been investigated, including statistical or inter-penetrating networks, nanocomposites, nanoparticle networks and core shell structures.[13-15]

In statistical network hydrogels, most common when various polymerizable monomers/crosslinkers are used to form a hydrogel, the distribution of comonomers and crosslinks is governed by the relative homo-propagation and cross-propagation rates of the various reactive building blocks. By varying the amount or type of monomers/crosslinkers added, properties can be tuned in correspondence to loosening or shrinking the network. However, many of these regular gels perform poorly to an applied stress and are relatively weak due to static crosslinks[16].

In order to improve the stress response of these hydrogels, many researchers have studied the incorporation of a dispersed phase into the hydrogel to create a hydrogel nanocomposite. By incorporating dispersed phases with dimensions on the nano length scale, optical properties such as transparency can be retained while still improving the stress response properties.[17] The dispersed phases used to form such nanocomposites range from inorganic materials like clays and minerals to organic materials such as starches and poly (lactic acid).[18-22] Specifically relevant to this thesis are previous examples in which starch is used as a filler. Although the incorporated planar starch nanocrystals gave better mechanical performance to tensile stress due to their stacked microstructure, the starch nanoparticles additive instead gave better macroscopic optical transparency due to their smaller size.[20]

Alternately, the use of discrete phases that can be degraded *in situ* without degrading the hydrogel network can lead to the formation of well-defined macroscopic pores in the continuous hydrogel

phase that offer advantageous properties for drug delivery, tissue engineering, or bioseparation applications.[23, 24] The use of naturally derived polysaccharides that naturally erode via enzymatic or hydrolytic pathways is particularly attractive in this context given that the by-products of such degradation events are typically cytocompatible small molecules such as sugars. Starch for example can be readily degraded into its monomers of glucose by digestion by α-amylase.[25-27] In a hydrogel matrix with starch grafted into the structure, the degradation of that building block can be effective in eliciting an engineered response, such as release of drugs which were entrapped in the starch.[28]

1.3 – Hydrogel Applications

Hydrogels have many practical applications which can solve issues currently faced in various fields,[29] including biotechnology (where they have been developed for use as mimetic tissue scaffolds),[3] agricultural applications (as vehicles for controlled delivery of payloads such as growth factors or pesticides),[30] and separation science, (where their porous structure can be applied to purify a mixture).[31] The use of hydrogels for tissue engineering has attracted particular recent interest. However, for hydrogels to be used in these areas effectively, they must have certain characteristics suitable for the application. For example, in 3D printing of hydrogel-based tissue scaffolds, inks are typically injectable and pressure driven from a controller. This inherently means the gel must have a tunable and relatively short curing time to enable network formation from a liquid ink within a matter of seconds between initial injection, initial deposition and redeposition of a fresh layer. The overall low cytotoxicity of the material, as well as any crosslinking process (particularly if it is intended to act *in situ* in the presence of tissues) and the eventual degradation products of the hydrogel, are also critical considerations. It is for this reason that many naturally occurring biopolymers have been investigated for tissue engineering applications, as they are generally cytocompatible and degrade into small biomolecules such as sugars or amino acids. The mechanical strength of a hydrogel is also essential to control in the context of tissue engineering since different tissues have different mechanical strengths; for example, brain tissue has a Young's

modulus of ~1 kPa while bone tissue has a modulus of ~100 kPa or more. It is important that a biomaterial is able to match the elasticity of the native tissue of that area to allow for successful outcomes while also ensuring minimal inflammatory responses at the site of injection.[6]

Key biological properties also have to be satisfied for fabricating successful tissue scaffolds, including successful cell proliferation and/or differentiation. PEG derived hydrogels prove to be suitable for use as artificial ECMs since they have low protein adsorption and can be modified for selective cellular adhesion. By incorporating anchoring peptide sequences such as arginylglycylaspartic acid (RGD), an integrin peptide responsible for cellular adhesion to the natural ECM, the interactivity of the gel with cells can be also tuned.[32, 33]

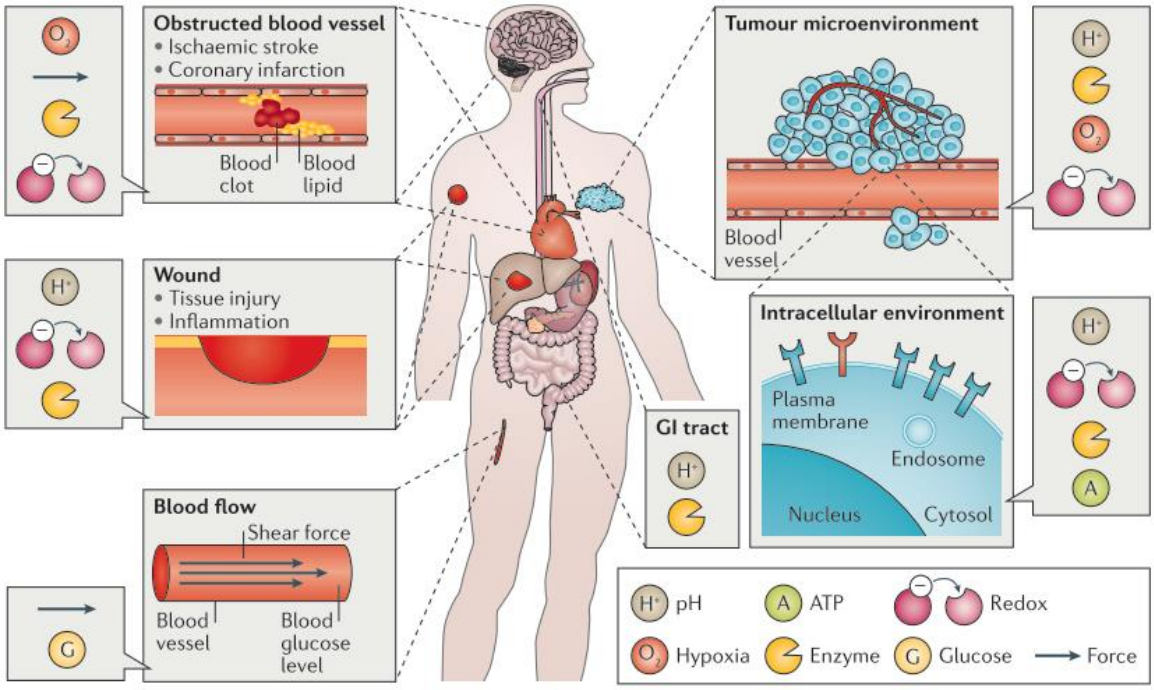

Figure 1-1. *Schematic of different microenvironments of the human body and their chemical stimuli (see symbol legend in bottom right corner). Adapted from Langer et al., Bioresponsive Materials in Nature Reviews: Materials, 2016.*[33]

The ability of a tissue scaffold to degrade at a rate complementary to the natural extracellular matrix (ECM) production by the cells in the developing tissue is a critical factor to the success of most hydrogels in tissue engineering applications. This ability is incorporated in hydrogel design in a variety of different ways. pH responsive reversible crosslinking is a common and popular strategy,

often using dynamic covalent chemistries such as hydrazone crosslinking (aldehyde + hydrazide) or charge-based crosslinking using pH-dependent cationic and anionic groups. Functionalized biopolymers can also be used as the crosslinker, as they have been shown to degrade by hydrolytic or enzymatic means.[25, 34-37] The approaches can also be combined by incorporating the mentioned crosslinking chemistries into natural biopolymers.[38, 39] Such crosslinking strategies would create a structure by which the mechanical properties are highly influenced by the incorporated biopolymer.

While dynamic covalent or physical crosslinking is most typically employed to enable minimally-invasive therapies, other approaches can be used to convert more conventional polymerization strategies into a biomedical workflow. In a series of papers by Khoushabi et al., a hydrogel-based treatment for chronic back pain attributed to tissue degeneration of the intervertebral disc was established, first by building a Monte Carlo model to assess the feasibility of such a tissue replacement by simulating the optical dynamics in vertebrae cavity[40] followed by developing a mechanically suitable injectable gel for this purpose (**Figure 1-2**). While photopolymerization was used as the gelation strategy, this technology qualified as minimally invasive due to the use of a fiber optic inserted into a joint carrying a prepolymer solution, meeting in the needle coaxially. This approach allows for extrusion of a prepolymer solution to a specified site while allowing for

polymerization of the solution *in situ*, enabling the delivery of the PEG-based hydrogel treatment to a degenerated disc and restoration of the original disc height.[40-42]

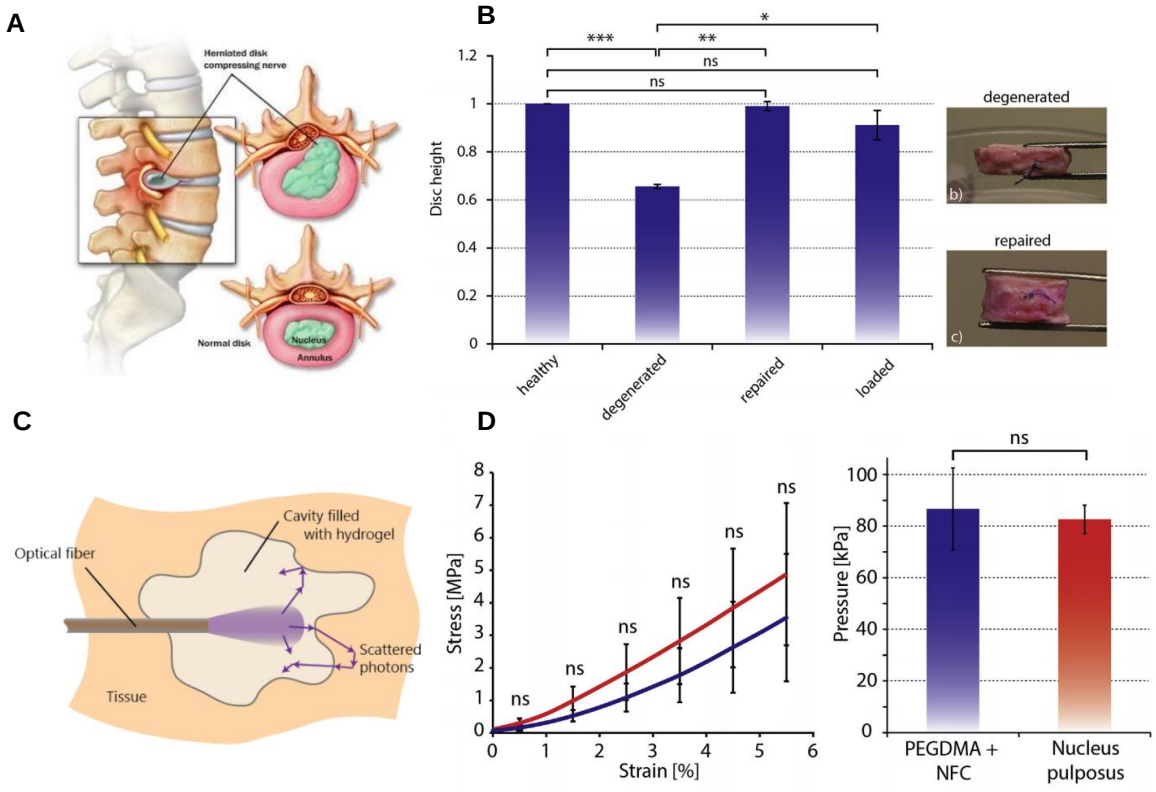

Figure 1-2. *Summary of work by Khoushabi et al.[39-41] using PEG based UV cured replacement of nucleus pulposus in intervertebral discs via injection. A. Anatomical comparison of a healthy intervertebral disc and a herniated discs impact on the nerve. B. Reported disc heights of healthy, degenerated, repaired and compression loaded discs (left), as well as optical images of degenerated and repaired discs (right). C. Schematic of optical fiber UV illumination of a tissue cavity via injection. D. Mechanical performance of the replacement PEGDMA+NFC scaffold vs. natural nucleus pulposus. Confined compression stress vs. strain curve (left) and the swelling pressure (right).*

While PEG-based hydrogels are likely the most widely investigated for tissue engineering applications and biomedical applications more broadly, POEGMA (poly(oligoethylene glycol methacrylate))-based polymers have more recently been investigated as complementary non-cytotoxic, protein-repellent “smart” materials. In particular, our group has extensively reported on POEGMA gels designed to be injectable *in situ* via twin extrusion of a hydrazone-crosslinking Oligo ethylene glycol methacrylate, molecular weight = 500g/mol ($OEGMA_{500}$) and di (ethylene glycol) methacrylate ($M(EO)_2MA$) copolymer. These extruded gels show no cytotoxic response on 3T3 cells, minimal inflammation *in vivo*, low protein adsorption to proteins such as bovine serum albumin

(BSA), and tunable elastic storage modulus based on concentration and functionality. These hydrogels can also degrade via the reversibility of the hydrazone bond under acidic conditions, proving to be a promising biomaterial as a tissue scaffold.[43, 44] These hydrogels have also been investigating for their drug delivery properties by taking advantage of their lower critical solution temperature (LCST) properties, tunable based on the molar ratio of $OEGMA_{500}$ and $M(EO)_2MA$ between 10-100% $OEGMA_{500}$ to create hydrogels with well-defined swelling, degradation, and mechanical properties.[45, 46] Such chemistry has also been applied in nanogel formulations by taking advantage of the LCST phenomenon to drive the self-assembly of crosslinked nanogels. An initial aldehyde or hydrazide functionalized template POEGMA polymer is brought to a temperature higher than its LCST, forcing it to collapse; a complementary functionalized polymer solution is then added to create hydrazone crosslinked nanogels. These nanogels are currently being investigated for use in drug delivery, as their size between 50-150 nm should allow for effective circulation.[47]

1.4 – Biopolymers

The three main types of biopolymers, polynucleic acids, polysaccharides and polypeptides, have all been well studied as building blocks for biomedical materials. The monomers which make up these chains are typically biologically relevant small molecules such as nucleic acids, sugars or amino acids respectively, and most biopolymers can readily degrade, whether by hydrolysis or enzymatically, back into these constituent monomers. In contrast, most synthetic polymers are either non-degradable or degrade into non-biological components. Biopolymers are also available with an abundance of chemical functionalization which can be used for conjugation of small molecules, enabling a wide range of functionality such as drug integration or the incorporation of crosslinking groups. In the case of polysaccharides specifically, the abundance of primary and secondary hydroxyl groups allows for several functional groups to be integrated. For example, the oxidation of vicinal diols in starches and dextran using 1 equivalent of sodium periodate yields 2 equivalents of aldehyde groups, although hemiacetal groups form when the chains are oxidized to greater than 25% of the monomer equivalents that can lead to negative effects such as decreased

or complete loss of solubility.[48] These aldehyde sites can be used for attachment of other molecules via various reactions such as imine Schiff base formation, which occurs spontaneously upon the addition of an aminated molecule and is highly reversable with pH. The imine bond can alternately be readily reduced using sodium cyanoborohydride to make it more permanent.

Functionalization of the carbohydrate chains with small molecules enables the production of further functionalized biopolymers; for example, reaction with chloroacetic acid results in carboxymethylation of the structure while the use of glycidyl methacrylate results in the tethering of methacrylate groups. These reactions typically happen at the C6 primary hydroxyl group, as it is free for rotation and is much less sterically hindered. Both functionalizations can be then used for other purposes, such as drug binding or polymer grafting.[49]

1.5 – Starch & Starch Nanoparticles

Starch is the most abundant polysaccharide on Earth, as it is made by various plants for long-term energy storage. It has been found in high abundance in waxy corn, rice and potatoes, among other sources. Chemically, it is a polymer made from monomers of glucose strung together by a α-[1,4]-

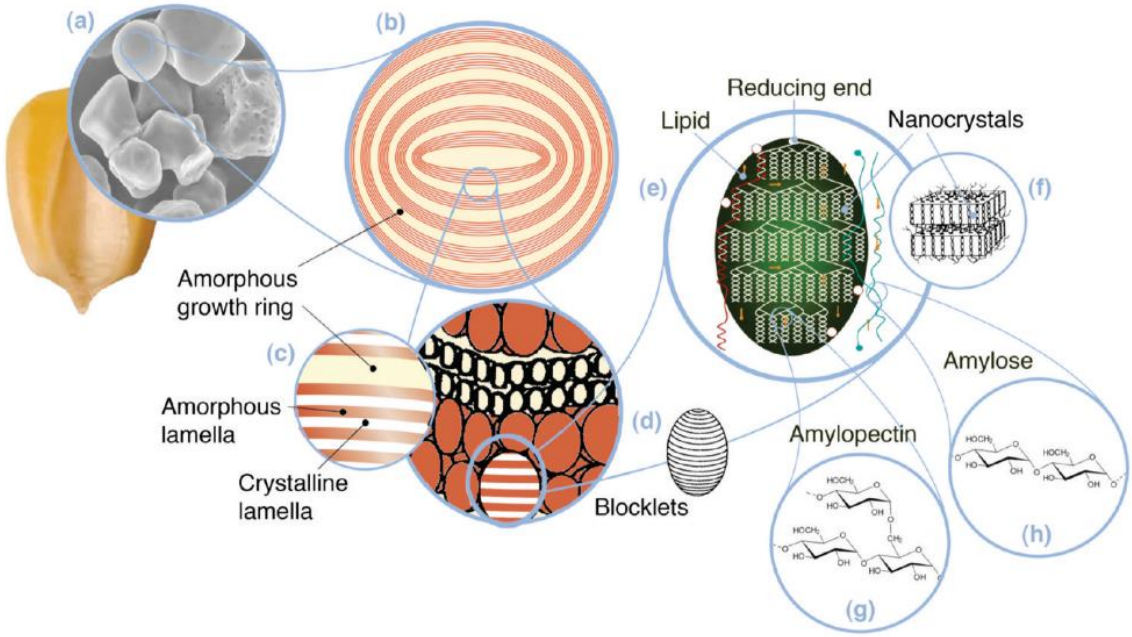

Figure 1-3. *Macro, micro and molecular structures of starch. Adapted from Le Corre et al. in Starch Nanoparticles: A Review in Biomacromolecules, 2010.*[57]

glycosidic linkages. These links can continue as linear, amorphous regions called amylose, or develop branching points via α-[1,6]-glycosidic linkages leading to crystalline domains called amylopectin (**Figure 1-3**). These crystalline domains are what allow starch to form granules which are birefringent.[50]

Depending on the plant source of the starch, its ratio of amylose/amylopectin regions can differ greatly. Due to these tightly bound structures, many starches are water insoluble, unless helped to dissolve using heat. This is typically defined as gelatinization, as increased temperature allows the penetration of water into the crystalline domains of amylopectin to loosen the molecular structure and ultimately lead to partial dissolution. However, when cooled back down, these structures typically reform into their granular structure, which is called retrogradation.[51-53] To mitigate retrogradation and allow the starch to keep its advantageous properties such as malleability, starch can be modified using a chemical plasticizer. Commonly used plasticizers are water, urea, glycerol and other small polar molecules which can be worked in to the starch and keep it from retrograding by inhibiting intramolecular hydrogen bonding.[54] By modifying the starch this way, it retains its desirable properties such as pliability when warmed and exhibits improved solubility. These improvements can be easily carried out in a reactive extruder, as high temperature, pressure and shear can be applied onto the starch while being mixed with a plasticizer. Such products have been used extensively as films and adhesives as biodegradable alternatives to synthetic plastics.[55-57]

Starch nanoparticles have been widely studied in the literature and have been shown as effective additives for nanocomposites and interesting macromolecules for drug delivery and tissue scaffold applications.[22, 58-60] In most cases, starch nanoparticles are formed via inverse emulsion-templated systems in which gelatinized starch is crosslinked inside the dispersed water phase to form a nanoparticle.[60-62] EcoSynthetix Inc. has been able to create starch nanoparticles with an average diameter in the 20-200 nm size range via a proprietary reactive extrusion method. The hot extrudate is then ground while water is evaporated, creating a granular brown powder. When resuspended in aqueous media, the water content of each SNP can be greater than 90%.

Commercially, these latexes are used in the pulp and paper industry as eco-friendly adhesives and additives in paper making. However, the biopolymer source and high water content of these SNPs offer promise for biomedical applications as well. In a recent study published in Advanced Materials by Lahann et al., these nanoparticles were chemically functionalized successfully to attach both a cationic charge (via reaction with glycidyl ammonium chloride in basic conditions) and a fluorescent tag (via TEMPO oxidation to generate a carboxylic acid group that can subsequently conjugate fluorescein amine using EDC/NHS). Application of this material on extracted teeth and indicated that the fluorescent SNPs are an effective indicator of carious lesions against healthy tooth tissue and against controls such as FITC-Dextran, FITC alone, a non-legion control, and an anionic analog.[65]

1.6 – Tissue Engineering & Void Forming Hydrogels

One of the many morphologies investigated as potentially suitable tissue scaffolds is the architecture of a void forming hydrogel.[66] These voids have been hypothesized as beneficial for the development of the ECM of proliferating cells within the gel, leading to positive outcomes for the tissue scaffold. An example of these void forming hydrogels was reported in Nature Materials by Huebsch et al., who used a predegraded alginate porogen and high molecular weight alginate bulk gel system summarized in **Figure 1-4**. The hydrogel was made by co-encapsulating mesenchymal stem cells and the fabricated oxidized alginate porogen inside a non-degraded alginate matrix. Over time, the predegraded porogen was observed to hydrolyze faster relative to the bulk gel, allowing the stem cells to proliferate while also allowing for drastic changes in the relative storage modulus of the gel as a function of porogen volume percentage. Using this change in mechanical strength, the authors were able to induce mechanotransduction pathways for the encapsulated mesenchymal stem cells to differentiate into regenerated bone tissue. This study highlights the

importance of using such biophysical signals to allow for transplanted-cell-mediated tissue repair to be a viable treatment.[67]

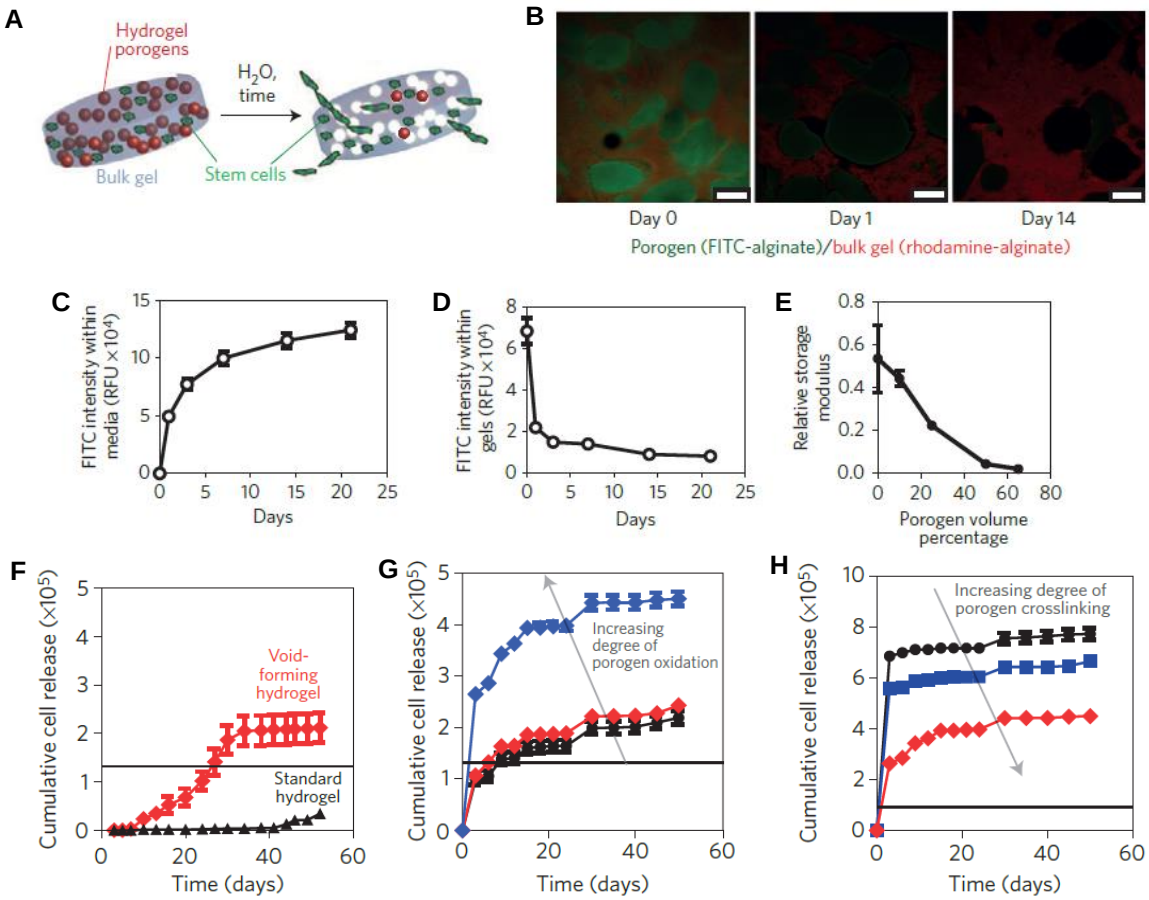

Figure 1-4. *Summary of results from Huebsch et al.[65] A. Schematic for porogen erosion and void formation in bulk gel, allowing for greatly cell proliferation. B. Confocal microscopy of fluorescently labelled porogen/bulk gels over time, showing porogen-FITC disappearing over time. C. FITC intensity of supernatant over time D. FITC intensity of gel over time. E. Study of shear modulus with increasing porogen volume percentage. F. Cell count on void forming vs. standard hydrogel. G. Cell count as a function of porogen oxidation. H. Cell count as a function of porogen crosslinking.*

1.7 – Thesis Objectives

The premise of this thesis was to investigate the synthesis, properties, and applications of a bulk hydrogel which can (1) physically entrap starch nanoparticles or (2) use starch nanoparticles as crosslinkers for constructing bio-based impregnated hydrogels. The secondary objective was to selectively erode the entrapped SNPs and study the effect of the resulting voids on hydrogel properties and performance. Hydrogels with this void morphology have previously been shown as

successful tissue scaffolds with exciting properties and applications in drug delivery; however, the uniquely small size of the SNPs produced by EcoSynthetix offer a particular opportunity in this research for creating nanoscale void domains that may impart useful functional properties.

In Chapter 2, a study of encapsulating starch nanoparticles in a UV-curable POEGMA matrix is described. Many parameters including as comonomer ratio, relative crosslinker amount and concentration of SNPs incorporated were varied to determine an optimal hydrogel formulation in terms of curing time, mechanical performance, and swellability. These nanocomposite gels were then subjected to degradation studies to probe the ability of the SNPs to be digested into degradation products such as oligomeric starch and monomeric glucose units. To facilitate this degradation, methods of both enzymatic and hydrolytic erosion were screened and quantified using selective assays for glucose and starch. The adsorption capacity of these gels for a model dye was also investigated before and after degradation to develop a better understanding of the effect of the generated increased porosity of the hydrogel internal structure.

Subsequently, in Chapter 3, the synthetic crosslinker ethylene glycol dimethacrylate (EGDMA) used in Chapter 2 was replaced with methacrylate functionalized starch nanoparticles (SNP-MA). Hypothetically, hydrogels formed with natural polymers as the crosslinker should allow for complete degradation by biologically relevant means (i.e. hydrolysis or enzymatic degradation). The mechanical properties, curing time and swelling capacity of the resulting hydrogels were first assessed, followed by an investigation on the consequences of SNP degradation by α-amylase on the gel properties over time.

Overall, this thesis aims to gain a better understanding of how the small size and degradability offered by SNPs can be leveraged in practical applications.

1.8 – References

1. Okay, O., General Properties of Hydrogels. In *Hydrogel Sensors and Actuators*, 2009; pp 1-14.
2. Patenaude, M.; Smeets, N. M.; Hoare, T., Designing injectable, covalently cross-linked hydrogels for biomedical applications. *Macromol. Rapid Commun.* **2014,** *35* (6), 598-617.
3. Brown, T. E.; Anseth, K. S., Spatiotemporal hydrogel biomaterials for regenerative medicine. *Chem. Soc. Rev.* **2017,** *46* (21), 6532-6552.
4. Van Nieuwenhove, I.; Van Vlierberghe, S.; Salamon, A.; Peters, K.; Thienpont, H.; Dubruel, P., Photo-crosslinkable biopolymers targeting stem cell adhesion and proliferation: the case study of gelatin and starch-based IPNs. *J. Mater. Sci. Mater. Med.* **2015,** *26* (2), 104.
5. Majcher, M. J.; Hoare, T., Hydrogel Synthesis and Design. In *Functional Biopolymers*, 2018; pp 1-41.
6. Khan, F.; Tanaka, M., Designing Smart Biomaterials for Tissue Engineering. *Int. J. Mol. Sci.* **2017,** *19* (1).
7. Koetting, M. C.; Peters, J. T.; Steichen, S. D.; Peppas, N. A., Stimulus-responsive hydrogels: Theory, modern advances, and applications. *Mater. Sci. Eng. R Rep.* **2015,** *93*, 1-49.
8. Poorgholy, N.; Massoumi, B.; Jaymand, M., A novel starch-based stimuli-responsive nanosystem for theranostic applications. *Int. J. Biol. Macromol.* **2017,** *97*, 654-661.
9. Qiu, Y.; Park, K., Environment-sensitive hydrogels for drug delivery. *Adv. Drug Del. Rev.* **2012,** *64*, 49-60.
10. Hamidi, M.; Azadi, A.; Rafiei, P., Hydrogel nanoparticles in drug delivery. *Adv Drug Deliv Rev* **2008,** *60* (15), 1638-49.
11. Nash, M. E.; Healy, D.; Carroll, W. M.; Elvira, C.; Rochev, Y. A., Cell and cell sheet recovery from pNIPAm coatings; motivation and history to present day approaches. *J. Mater. Chem.* **2012,** *22* (37), 19376-19389.
12. Wang, L. L.; Wu, Y.; Men, Y. J.; Shen, J. N.; Liu, Z. P., Thermal-sensitive Starch-g-PNIPAM prepared by Cu(0) catalyzed SET-LRP at molecular level. *Rsc Advances* **2015,** *5* (87), 70758-70765.
13. Yang, J. L.; Gao, C. M.; Lu, S. Y.; Wang, X. G.; Chen, M. J.; Liu, M. Z., Novel self-assembled amphiphilic mPEGylated starch-deoxycholic acid polymeric micelles with pH-response for anticancer drug delivery. *Rsc Advances* **2014,** *4* (98), 55139-55149.
14. Xia, X.; Hu, Z.; Marquez, M., Physically bonded nanoparticle networks: a novel drug delivery system. *J. Control. Release* **2005,** *103* (1), 21-30.
15. Zhu, B.; Ma, D.; Wang, J.; Zhang, S., Structure and properties of semi-interpenetrating network hydrogel based on starch. *Carbohydr. Polym.* **2015,** *133*, 448-55.
16. Majcher, M. J.; Hoare, T., Advanced Hydrogel Structures. In *Functional Biopolymers*, 2018; pp 1-27.
17. Haraguchi, K., Nanocomposite hydrogels. *Curr. Opin. Solid State Mater. Sci.* **2007,** *11* (3-4), 47-54.
18. Jamshidian, M.; Tehrany, E. A.; Imran, M.; Jacquot, M.; Desobry, S., Poly-Lactic Acid: Production, Applications, Nanocomposites, and Release Studies. *Comprehensive Reviews in Food Science and Food Safety* **2010,** *9* (5), 552-571.
19. Haraguchi, K.; Takehisa, T., Nanocomposite hydrogels: A unique organic-inorganic network structure with extraordinary mechanical, optical, and swelling/de-swelling properties. *Adv. Mater.* **2002,** *14* (16), 1120-1124.
20. Bel Haaj, S.; Thielemans, W.; Magnin, A.; Boufi, S., Starch nanocrystals and starch nanoparticles from waxy maize as nanoreinforcement: A comparative study. *Carbohydr. Polym.* **2016,** *143*, 310-7.
21. Gomes, R. F.; de Azevedo, A. C.; Pereira, A. G.; Muniz, E. C.; Fajardo, A. R.; Rodrigues, F. H., Fast dye removal from water by starch-based nanocomposites. *J. Colloid Interface Sci.* **2015,** *454*, 200-9.

22. Le Corre, D.; Angellier-Coussy, H., Preparation and application of starch nanoparticles for nanocomposites: A review. *React. Funct. Polym.* **2014,** *85*, 97-120.
23. Mun, S.; Kim, Y. R.; McClements, D. J., Control of beta-carotene bioaccessibility using starch-based filled hydrogels. *Food Chem.* **2015,** *173*, 454-61.
24. Mun, S.; Kim, Y. R.; Shin, M.; McClements, D. J., Control of lipid digestion and nutraceutical bioaccessibility using starch-based filled hydrogels: Influence of starch and surfactant type. *Food Hydrocolloids* **2015,** *44*, 380-389.
25. Azevedo, H. S.; Gama, F. M.; Reis, R. L., In vitro assessment of the enzymatic degradation of several starch based biomaterials. *Biomacromolecules* **2003,** *4* (6), 1703-1712.
26. Goldbart, R.; Traitel, T.; Lapidot, S. A.; Kost, J., Enzymatically controlled responsive drug delivery systems. *Polym. Adv. Technol.* **2002,** *13* (10-12), 1006-1018.
27. Lu, D. R.; Xiao, C. M.; Xu, S. J., Starch-based completely biodegradable polymer materials. *Express Polymer Letters* **2009,** *3* (6), 366-375.
28. Simi, C. K.; Emilia Abraham, T., Hydrophobic grafted and cross-linked starch nanoparticles for drug delivery. *Bioprocess Biosyst. Eng.* **2007,** *30* (3), 173-80.
29. Harrison, R. H.; Steele, J. A.; Chapman, R.; Gormley, A. J.; Chow, L. W.; Mahat, M. M.; Podhorska, L.; Palgrave, R. G.; Payne, D. J.; Hettiaratchy, S. P.; Dunlop, I. E.; Stevens, M. M., Modular and Versatile Spatial Functionalization of Tissue Engineering Scaffolds through Fiber-Initiated Controlled Radical Polymerization. *Adv. Funct. Mater.* **2015,** *25* (36), 5748-5757.
30. Lu, Y.; Aimetti, A. A.; Langer, R.; Gu, Z., Bioresponsive materials. *Nature Reviews Materials* **2016,** *2* (1).
31. Alberta Araújo, M.; Cunha, A. M.; Mota, M., Enzymatic degradation of starch-based thermoplastic compounds used in protheses: identification of the degradation products in solution. *Biomaterials* **2004,** *25* (13), 2687-2693.
32. Cai, X.; Yang, L.; Zhang, L. M.; Wu, Q., Evaluation of amylose used as a drug delivery carrier. *Carbohydr. Res.* **2010,** *345* (7), 922-8.
33. Hong, Y.; Song, H.; Gong, Y.; Mao, Z.; Gao, C.; Shen, J., Covalently crosslinked chitosan hydrogel: properties of in vitro degradation and chondrocyte encapsulation. *Acta Biomater.* **2007,** *3* (1), 23-31.
34. Kharkar, P. M.; Kiick, K. L.; Kloxin, A. M., Designing degradable hydrogels for orthogonal control of cell microenvironments. *Chem. Soc. Rev.* **2013,** *42* (17), 7335-72.
35. Agrawal, S. K.; Sanabria-DeLong, N.; Tew, G. N.; Bhatia, S. R., Nanoparticle-Reinforced Associative Network Hydrogels. *Langmuir* **2008,** *24* (22), 13148-13154.
36. Al-Itry, R.; Lamnawar, K.; Maazouz, A., Biopolymer Blends Based on Poly (lactic acid): Shear and Elongation Rheology/Structure/Blowing Process Relationships. *Polymers* **2015,** *7* (5), 939-962.
37. Wax, A.; Backman, V.; Schmocker, A. M.; Khoushabi, A.; Gantenbein-Ritter, B.; Chan, S.; Bonél, H. M.; Bourban, P.-E.; Månson, J. A.; Schizas, C.; Pioletti, D.; Moser, C., Minimally invasive photopolymerization in intervertebral disc tissue cavities. In *Biomedical Applications of Light Scattering VIII*, 2014.
38. Khoushabi, A.; Schmocker, A.; Pioletti, D. P.; Moser, C.; Schizas, C.; Manson, J. A.; Bourban, P. E., Photo-polymerization, swelling and mechanical properties of cellulose fibre reinforced poly(ethylene glycol) hydrogels. *Compos. Sci. Technol.* **2015,** *119*, 93-99.
39. Schmocker, A.; Khoushabi, A.; Frauchiger, D. A.; Gantenbein, B.; Schizas, C.; Moser, C.; Bourban, P. E.; Pioletti, D. P., A photopolymerized composite hydrogel and surgical implanting tool for a nucleus pulposus replacement. *Biomaterials* **2016,** *88*, 110-9.
40. Bakaic, E.; Smeets, N. M. B.; Hoare, T., Injectable hydrogels based on poly(ethylene glycol) and derivatives as functional biomaterials. *Rsc Advances* **2015,** *5* (45), 35469-35486.
41. Smeets, N. M.; Bakaic, E.; Patenaude, M.; Hoare, T., Injectable and tunable poly(ethylene glycol) analogue hydrogels based on poly(oligoethylene glycol methacrylate). *Chem. Commun. (Camb.)* **2014,** *50* (25), 3306-9.

42. Bakaic, E.; Smeets, N. M. B.; Dorrington, H.; Hoare, T., “Off-the-shelf” thermoresponsive hydrogel design: tuning hydrogel properties by mixing precursor polymers with different lower-critical solution temperatures. *RSC Advances* **2015,** *5* (42), 33364-33376.
43. Smeets, N. M.; Bakaic, E.; Patenaude, M.; Hoare, T., Injectable poly(oligoethylene glycol methacrylate)-based hydrogels with tunable phase transition behaviours: physicochemical and biological responses. *Acta Biomater.* **2014,** *10* (10), 4143-55.
44. Simpson, M. J.; Corbett, B.; Arezina, A.; Hoare, T., Narrowly Dispersed, Degradable, and Scalable Poly(oligoethylene glycol methacrylate)-Based Nanogels via Thermal Self-Assembly. *Ind. Eng. Chem. Res.* **2018,** *57* (22), 7495-7506.
45. Maia, J.; Carvalho, R. A.; Coelho, J. F. J.; Simoes, P. N.; Gil, M. H., Insight on the periodate oxidation of dextran and its structural vicissitudes. *Polymer* **2011,** *52* (2), 258-265.
46. Hermanson, G. T., *Bioconjugate Techniques*. 3rd ed.; Elsevier Inc.: 2013.
47. Ismail, H.; Irani, M.; Ahmad, Z., Starch-Based Hydrogels: Present Status and Applications. *International Journal of Polymeric Materials and Polymeric Biomaterials* **2013,** *62* (7), 411-420.
48. Athawale, V. D.; Lele, V., Thermal studies on granular maize starch and its graft copolymers with vinyl monomers. *Starch-Starke* **2000,** *52* (6-7), 205-213.
49. Li, T. X.; Li, K.; Wang, Y. M.; Su, H. B.; Wang, Q.; Cui, H. Z., Effects of gelatinization characteristics on starch-based superabsorbent polymer. *Mater. Res. Innovations* **2015,** *19* (sup5), 817-821.
50. Sarazin, P.; Li, G.; Orts, W. J.; Favis, B. D., Binary and ternary blends of polylactide, polycaprolactone and thermoplastic starch. *Polymer* **2008,** *49* (2), 599-609.
51. Ma, X. F.; Yu, J. G.; Wan, J. J., Urea and ethanolamine as a mixed plasticizer for thermoplastic starch. *Carbohydr. Polym.* **2006,** *64* (2), 267-273.
52. Arrieta, M. P.; Samper, M. D.; Aldas, M.; Lopez, J., On the Use of PLA-PHB Blends for Sustainable Food Packaging Applications. *Materials (Basel)* **2017,** *10* (9).
53. Dou, Y.; Huang, X.; Zhang, B. N.; He, M.; Yin, G. Q.; Cui, Y. D., Preparation and characterization of a dialdehyde starch crosslinked feather keratin film for food packaging application. *Rsc Advances* **2015,** *5* (34), 27168-27174.
54. Zhai, M. L.; Yoshii, F.; Kume, T., Radiation modification of starch-based plastic sheets. *Carbohydr. Polym.* **2003,** *52* (3), 311-317.
55. Deborah Le Corre, J. B., and Alain Dufresne, Starch Nanoparticles: A Review. *Biomacromolecules* **2010,** *11* (5), 15.
56. Tan, Y.; Wang, P. X.; Xu, K.; Li, W. B.; An, H. Y.; Li, L. L.; Liu, C.; Dong, L. S., Designing Starch-Based Nanospheres to Make Hydrogels with High Mechanical Strength. *Macromolecular Materials and Engineering* **2009,** *294* (12), 855-859.
57. Zhou, G.; Luo, Z.; Fu, X., Preparation of starch nanoparticles in a water-in-ionic liquid microemulsion system and their drug loading and releasing properties. *J. Agric. Food Chem.* **2014,** *62* (32), 8214-20.
58. Chakraborty, S.; Sahoo, B.; Teraoka, I.; Gross, R. A., Solution properties of starch nanoparticles in water and DMSO as studied by dynamic light scattering. *Carbohydr. Polym.* **2005,** *60* (4), 475-481.
59. Blasco, C.; Pico, Y., Determining nanomaterials in food. *Trac-Trends in Analytical Chemistry* **2011,** *30* (1), 84-99.
60. Jones, N. A.; Chang, S. R.; Troske, W. J.; Clarkson, B. H.; Lahann, J., Nanoparticle-Based Targeting and Detection of Microcavities. *Adv Healthc Mater* **2017,** *6* (1).
61. Salvati, A.; Soderman, O.; Lynch, I., Plum-pudding gels as a platform for drug delivery: Understanding the effects of the different components on the diffusion behavior of solutes. *J. Phys. Chem. B* **2007,** *111* (25), 7367-7376.
62. Huebsch, N.; Lippens, E.; Lee, K.; Mehta, M.; Koshy, S. T.; Darnell, M. C.; Desai, R. M.; Madl, C. M.; Xu, M.; Zhao, X.; Chaudhuri, O.; Verbeke, C.; Kim, W. S.; Alim, K.; Mammoto, A.; Ingber, D. E.; Duda, G. N.; Mooney, D. J., Matrix elasticity of void-forming hydrogels controls transplanted-stem-cell-mediated bone formation. *Nat Mater* **2015,** *14* (12), 1269-77.

2 Physically Entrapped Starch Nanoparticles in Ultraviolet-Cured Poly (Oligoethylene Glycol Methyl Ether Methacrylate) Hydrogels

2.1 - Introduction & Objectives

Nanocomposite hydrogels can be made by incorporating a dispersed phase into a prepolymer solution and stimulating polymerization either around or in conjunction with the dispersed phase to immobilize the dispersed phase within the continuous bulk hydrogel phase. Due to their small sizes, a variety of different nanoparticles can be effectively used as additives without compromising (or in some cases enhancing) key hydrogel properties including mechanics,[38] swelling capacity[18] and optical transparency.[20]

Poly (oligo ethylene glycol methacrylate) (POEGMA) hydrogels have been extensively studied both within our group and elsewhere as an attractive polymer for tissue engineering and drug delivery applications. POEGMA hydrogels are non-cytoxic and protein-repellent, providing key properties for cell-contacting applications.[46] These polymers also show lower critical solution temperature thermoresponsive behaviour depending on the monomer ratio of long chain oligoethylene glycol methacrylate (MW=500 g/mol) to short chain di (ethylene glycol) methacrylate ($M(EO)_2MA$), with hydrogels containing higher $M(EO_2)MA$ fractions de-swelling at lower temperatures. Such transitions, which drive the expulsion of water from the hydrogel network together with any entrapped/encapsulated therapeutic, have been widely studied for drug delivery applications.[43, 68]

POEGMA hydrogel nanocomposites have been previously studied in our group in collaboration with the Cranston group by incorporating cellulose nanocrystals (CNCs) into the POEGMA matrix. All the beneficial properties of POEGMA were maintained such as non-cytotoxicity, while drastic increases in the mechanical properties were achieved due to the presence of the rigid CNCs.[69]

Although most aspects of these gels are tunable including gel swelling and degradation, the use of CNCs may pose challenges with degradation when used *in vivo*.

Soft discrete phases such as microgels have also been used as entrapped phases within hydrogels. These types of soft composite gels have been typically developed for advanced drug delivery methods, in which the discrete microgel phase (a) alters the drug affinity to effect long-term release or (b) is released upon degradation of the bulk gel, allowing for circulation of drug filled responsive microgels if implanted in the body. Such a gel was previously reported by our group in which poly(N-isopropylacrylamide-co-acrylic acid) (pNIPAM-co-AA) microgels were used as entrapped phases inside an *in-situ* crosslinking hydrogel network made from aldehyde functionalized oxidized dextran and hydrazide functionalized carboxy methyl cellulose to enhance the drug affinity with the cationic drug bupivacaine. Due to the significantly higher partitioning of drug inside the microgel phase relative to the bulk hydrogel phase, these composite gels enabled significantly sustained release relative to each individual phase alone, showing effective release over 60 days when incorporated together compared to under 1 week with an initial burst release individually.[70]

Instead of the nanoscale discrete phase being used as a functional material, it can also be used as a template for the creation of pores inside a gel. Such an additive approach has been applied to generate various types of pores in hydrogels. Zenobi-Wang et al. described a macroporous hydrogel created around a dextran-based polysaccharide phase by taking advantage of the two-phase aqueous separation of dextran and poly(ethylene glycol) (PEG) as the PEG phase was polymerized. Pores of various sizes were produced depending on the concentration of the initial dextran solution, with solutions containing 0% -20% dextran creating porosities in the range of 0.50-50 µm respectively. The optimal formulation had a storage modulus of 70 Pa, which while appropriate for the described application for culturing neural cells from the encapsulated precursor dorsal root ganglia to create a functional neural network within the synthetic gel[71] is much too weak for most hydrogel applications. Huebsch et al. reported an alternate approach by encapsulating predegraded dialdehyde low molecular weight calcium-crosslinked alginate porogen beads inside

a high molecular weight calcium-crosslinked bulk alginate phase. The lower degree of crosslinking inside the discrete alginate phase enabled faster degradation of the discrete phase to create pores, as demonstrated by the associated decrease in mechanical performance and increase in mesenchymal stem cell proliferation within the gel that was leveraged for bone regeneration (i.e. the decrease in mechanical strength coupled with increase in porosity allows for the proliferating cells to undergo mechanotransduction differentiation pathways into osteoblasts).[67, 72] However, the pores generated by such an approach are on the size range of tens to hundreds of microns. To-date, there are few strategies available to create nanoporosity within gel networks using a discrete phase templating approach. The generation of such a nanoporous network would be of significant interest in the context of enhancing diffusion into a gel while excluding cellular components (e.g. for cell encapsulation applications), creating free volume to accelerate gel responses to the environment, and/or controlling the permeability of a gel layer for specific applications (e.g. the separation and capture of possible toxins and/or dyes from waste water[21]).

Starch nanoparticles (SNPs) are crosslinked networks of starch which are <100 nm in size.[58] They can be made by several methods and with different properties depending on the plant source, with their properties varying based on the processing conditions as well as the ratios of crystalline domains of branched amylopectin (which features branch points between the C1 and C6 carbons, specifically named α-[1,6]-glycosidic linkages) versus amorphous domains of linear amylose (linear strands of glucose monomers connected by an α-[1,4]-glycosidic linkage).[73] The SNPs created by EcoSynthetix are produced via a thermoplastic modification process in a reactive extruder.[74] The resultant blend is then cryoground, producing SNPs of 20-200 nm in size but a dominant fraction on the 20-50 nm diameter range.[63] SNPs can be readily modified and functionalized to facilitate different properties, such as charge, thermoresponsiveness or the capacity for self-association (e.g. via incorporation of long alkyl groups).[73, 75-77] These particles have been studied previously as effective biomaterials in the dental field for when modified for the detection of microcavities on teeth by fluorescence.[65]

There are two clear benefits to using SNPs as pore-forming templates for nanocomposite hydrogels: (1) SNPs can be enzymatically eroded, leaving behind voids in a monolithic hydrogel structure. Specifically, α-amylase has been shown to degrade similar materials by breaking down the α-[1,4]-glycosidic linkages holding each monomer together,[78, 79] with some reports also indicating that encapsulating the enzyme can allow for triggered degradation over time.[80] (2) SNPs are extremely small, with a dominant fraction on the size range of 20-50 nm. Thus, relative to previous soft extractable templates, the resulting pores following SNP degradation are much smaller, facilitating potential transport benefits as outlined earlier.

In this chapter, the physical impregnation of SNPs into UV-activated poly (oligoethylene glycol) methacrylate (POEGMA) bulk hydrogels to create a "plum pudding" nanocomposite morphology was investigated. The effects of SNP incorporation on performance of the gel as well as the potential to selectively degrade the SNPs from the gel to create a macroporous structure were then investigated, as per **Scheme 1**.

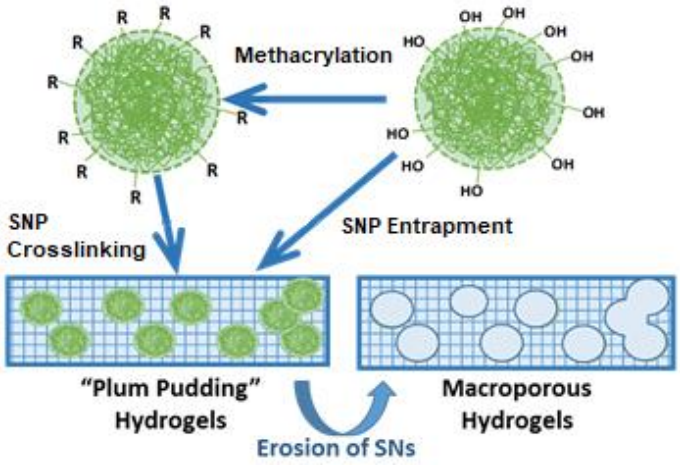

Scheme 2-1. *Schematic of approach used for using SNPs to generate plum pudding and macroporous hydrogels.*

The bulk hydrogel used for this work is shown in **Scheme 2**. Initiated by 365 nm ultraviolet (UV) light, the photoinitiator Irgacure 2959 produces a benzoyl radical and alkyl radical. These radicals will initiate the copolymerization of oligoethylene glycol methacrylate (MW=500 g/mol) [$OEGMA_{500}$] and methyl diethylene glycol methacrylate ($M(EO)_2MA$) and together with the difunctional crosslinker ethylene glycol dimethacrylate (EGDMA) to create a random statistical network gel. SNP-impregnated hydrogels can be produced by simply pre-mixing SNPs into the prepolymer solution.

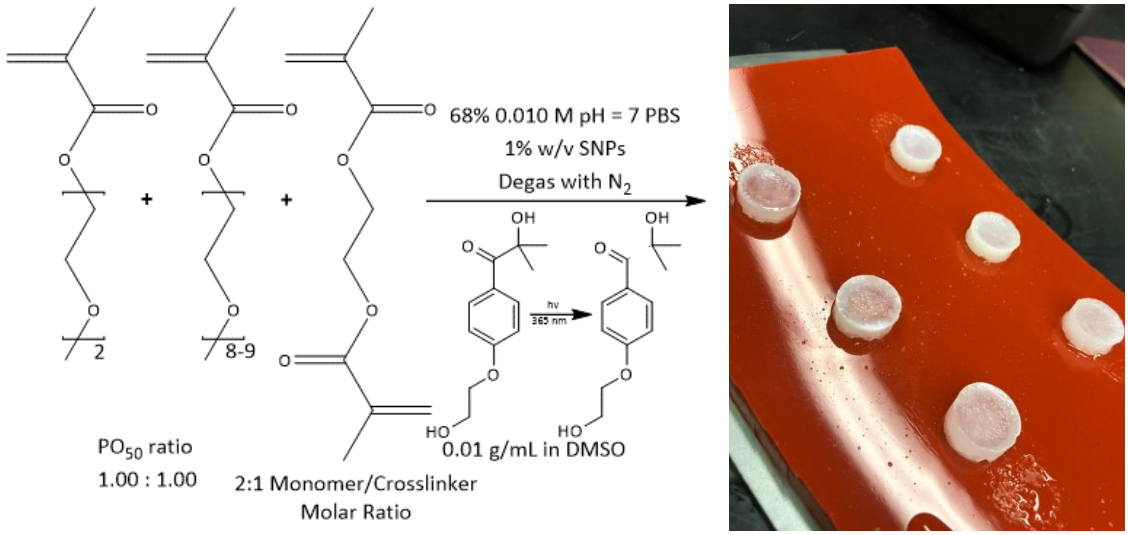

Scheme 2-2. *Synthetic method for creating UV-POEGMA hydrogels, with the resultant gels as an optical image.*

2.1.1 - Summary Chapter Objectives

In summary, the distilled objectives of this chapter are:

- To synthesize an ultraviolet-curable hydrogel matrix which can entrap SNPs
- To perform performance testing and material optimization by studying key parameters affecting gel properties
- To selectively degrade SNPs to create macroporous structures and characterize the properties of the new macroporous hydrogel materials.

2.2 - Materials

Experimental grade starch nanoparticles (SNPs) were made and donated by EcoSynthetix Inc. [Burlington, Ontario].

Poly (ethylene glycol) methyl ether methacrylate with an average molecular weight of 500 g/mol ($OEGMA_{500}$), di(ethylene glycol) methyl ether methacrylate ($M(EO)_2MA$), and ethylene glycol dimethacrylate (EGDMA) [MilliporeSigma, Oakville, Ontario] were filtered individually through basic alumina [Fisher Scientific, New Jersey] to remove the 4-methoxyphenol added as an inhibitor of auto-polymerization. Purified monomers were stored separately at 4°C until use.

Phosphate buffered saline tablets (PBS, 0.01 M phosphate buffer, 0.0027 M potassium chloride and 0.137 M sodium chloride, pH 7.4, at 25 °C) [MilliporeSigma, Oakville, Ontario] were dissolved in 200 mL/tablet of ultrapure Milli-Q grade deionized water (Milli-Q H_2O) to achieve the desired concentrations. The pH of the buffer was checked using a calibrated pH probe.

Glucose-Hexokinase (HK) Assay Kit was used as described in a technical bulletin from Sigma-Aldrich [MilliporeSigma, Oakville, Ontario]. 20 mL of Milli-Q H_2O was added to the assay vial to create a solution of 1.5 mM nicotinamide adenine dinucleotide (NAD), 1.0 mM adenosine triphosphate (ATP), 1.0 unit/mL of hexokinase (HK), and 1.0 unit/mL of glucose 6-phosphate dehydrogenase (G6P).

Deuterium oxide (D_2O) [10 x 1mL ampoules, 99.96% D from Cambridge Isotope Labs, Andover, Massachusetts], hydrochloric acid (HCl) [0.1 M, 1.0 M solutions from LabChem, Pennsylvania], sodium hydroxide (NaOH) [0.1 M, 1.0 M solutions from LabChem, Pennsylvania], sodium periodate ($NaIO_4$), 99% [AK Scientific, California], diethylene glycol [MilliporeSigma, Oakville, Ontario], fluorescein isothiocyanate isomer I (FITC) [MilliporeSigma, Oakville, Ontario], 2-hydroxy-4′-(2-hydroxyethoxy)-2-methylpropiophenone (Irgacure 2959) [MilliporeSigma, Oakville, Ontario], dimethyl sulfoxide (DMSO) [Caledon Laboratory Chemicals, Georgetown, Ontario], potassium iodide, 99% (KI) [ReagentPlus, MilliporeSigma, Oakville, Ontario], iodine, ≥ 99.8% (I_2) [ACS

reagent, MilliporeSigma, Oakville, Ontario], trifluoroacetic acid [Caledon Laboratory Chemicals, Georgetown, Ontario] and α-amylase [from bacillus subtilis, ~165,000 BAU/g, MP Biomedicals] were used as received and stored in appropriate conditions.

2.3 - Experimental Methods

2.3.1 - Modifications of Experimental Grade Starch Nanoparticles

2.3.1.1 - Dialysis of Starch Nanoparticles

To remove the potential complicating effects of small molecule additives used for SNP processing on enzymatic SNP degradation and bulk network formation, an aqueous dispersion of experimental grade SNPs (10%w/v in Milli-Q H_2O, pH = 7) was dialyzed using a membrane with a molecular weight cut off (MWCO) of 3.5 kDa over at least 6 cycles using Milli-Q H_2O over 3 days. Following, the SNPs were lyophilized to dryness and stored at room temperature. A 40 mg sample was dissolved in 1 mL deuterium oxide and the proton nuclear magnetic resonance (^{1}H NMR) spectrum was acquired using a Bruker AV 600 MHz spectrometer including water signal suppression. This product was denoted by “D-SNP”, specifying that it was dialyzed.

2.3.1.2 - Synthesis of Partially Degraded Dialdehyde Starch Nanoparticles

This protocol was adapted from Maia et al.[48, 49, 81] A 30.0 g aqueous dispersion of experimental grade SNPs (12.5% w/v in Milli-Q H_2O) was reacted with a 55 mL solution of $NaIO_4$ (dissolved at a mass of between 1.820 g to 9.102 g depending on the desired degree of substitution between 0.10-0.50 of anhydrous glucose units [AGUs]) in a darkened flask in order to minimize radical formation. The reaction was stirred for 4 hours, at which point an equimolar amount of ethylene glycol was added to quench any remaining periodate ions. The reaction was stirred overnight, followed by extensive dialysis using a 3.5 kDa MWCO membrane for 6x6+ hour dialysis cycles against Milli-Q H_2O. The product was then lyophilized, stored at room temperature in the dark, and characterized by ^{1}H NMR spectroscopy as described in 2.3.1.1. These products were denoted as “SNP-Ald-x”, where x was used to specify the degree of substitution of the pre-degraded SNPs.

2.3.1.3 - Synthesis of Fluorescein Isothiocyanate Isomer I Labeled Starch Nanoparticles

5.0 g of experimental grade SNPs were dissolved in 1.0 L of sodium carbonate buffer (0.5%w/v in 0.1 M, pH = 9.7) and reacted with 60.0 mg of fluorescein isothiocyanate isomer I for 18-24 hours in a darkened flask covered with aluminum foil. The product was dialyzed using a MWCO 3.5 kDa dialysis membrane against Milli-Q H_2O in the dark continuously until no fluorescence was detected in the dialysate, after which one more dialysis cycle was performed to ensure complete removal of unbound FITC. The purified mixture was then lyophilized and stored at room temperature in the dark. These products were denoted as "SNP-FITC".

2.3.2 - Synthesis of Physically Entrapped Starch Nanoparticles in Ultraviolet-Cured Poly (Oligoethylene Glycol Methyl Ether Methacrylate) Hydrogels

2.3.2.1 - Ultraviolet Cured Poly (Oligoethylene Glycol Methyl Ether Methacrylate) Hydrogels

This protocol was developed based on protocols from Khoushabi et al.[40-42] and Bakaic et al.[46] 1 g of $OEGMA_{500}$ (2 mmol), an equimolar amount $M(EO)_2MA$ comonomer (0.376 g, 2 mmol), and EGDMA crosslinker (0.396 g, 2 mmol) were mixed with 0.669 mL of a 0.01 g/mL dimethyl sulfoxide (DMSO) solution of Irgacure 2959 and diluted to 68%v/v using 5.02 mL of 0.01 M PBS. The solution was mixed well using a vortex mixer under nitrogen purging for ~30 minutes to create an inert atmosphere. The solution was then exposed to 365 nm ultraviolet light for 20 minutes in a Con-Trol-Cure Cure Zone 2 UV Flood Curing System equipped with a 400 W metal halide light source that outputs 80 mW/cm^2 of 365 nm long wave ultraviolet light.

2.3.2.2 - Ultraviolet Cured Poly (Oligoethylene Glycol Methyl Ether Methacrylate) Hydrogels with Physically Entrapped Starch Nanoparticles

To entrap SNPs in the hydrogel matrix outlined in section 2.3.2.1, SNPs were first suspended in 0.01 M PBS; after this suspension was used to dilute the hydrogel monomers, the SNPs were further dispersed at concentrations between 0.1-10% w/v using a vortex mixer. This method was used to entrap undialyzed SNPs (unD-SNPs), dialyzed SNPs (D-SNPs), predegraded aldehyde SNPs at a degree of substitution of 0.50 (SNP-Ald-0.50), and FITC-labeled SNPs (SNP-FITC). The

degree of substitution of aldehyde SNPs is twice proportional to oxidizing 25% of the anhydrous glucose units, producing 2 aldehyde groups each.

2.3.2.3 - PO_x Series of Ultraviolet Cured Poly (Oligoethylene Glycol Methyl Ether Methacrylate) Hydrogels with Physically Entrapped Starch Nanoparticles

Adapted from the work of Bakaic et al.[46], this study was performed to investigate the effect of varying the side chain length of the POEGMA precursor monomers that regulates the volume phase transition temperature of the bulk hydrogels. The same method outlined in section 2.3.2.2 was used to prepare the hydrogels but altering the $OEGMA_{500}$:$M(EO)_2MA$ ratio to create hydrogels labeled as PO_0 (4 mmol of $M(EO)_2MA$, no $OEGMA_{500}$), PO_{50} (2 mmol of $M(EO)_2MA$, 2 mmol of $OEGMA_{500}$) and PO_{100} (4 mmol of $OEGMA_{500}$, no $M(EO)_2MA$). Undialyzed SNPs were used as the entrapped phase for these experiments.

2.3.2.4 - Crosslinker Series of Ultraviolet Cured Poly (Oligoethylene Glycol Methyl Ether Methacrylate) Hydrogels with Physically Entrapped Starch Nanoparticles

This study was performed to investigate the effect of varying the molar ratio of the crosslinker EGDMA to the total number of moles of (monofunctional) monomers used to prepare the hydrogel matrix. The same recipe described in section 2.3.2.2 was used but the EGDMA amount used was changed to half (1 mM) or double (4 mM) that used in the base formulation. Undialyzed SNPs were again used as the entrapped phase.

2.3.3 - Ultraviolet Curing Rheology

Rheology experiments of precursor solutions and the rheological responses during gelation under UV light were conducted using a TA Instruments Discovery Hybrid Rheometer Mark 2 equipped with a UV accessory that allows for a 20 mm quartz plate to be used as the bottom plate for parallel plate testing, permitting for the precursor solution to be exposed to ultraviolet radiation and analyzed *in situ* during the photopolymerization process. The light source is an Excelitas Omnicure S2000 UV mercury light bulb with a maximum output of 300 mW/cm^2 at 365 nm. Light output is guided using a 5 mm fiber output light guide to the UV accessory, which subsequently directs the light upwards to the sample through the quartz plate.

A viscosity sweep was done on the precursor solution, after which the light source was turned on and the gelation kinetics were tracked by oscillatory rheology measurements over the course of photopolymerization. At the end of the irradiation time (120 seconds), the resultant gel structure was then further investigated using a strain sweep to identify the linear viscoelastic range followed by a frequency sweep to provide accurate assessments of the storage and loss moduli of the resulting hydrogels.

2.3.3.1 - Optimizing Water Content

Blank poly (oligoethylene glycol methyl ether methacrylate) hydrogels (prepared using the base recipe described in section 2.3.2.1) were fabricated with increasing amounts percentages of water (0%, 8%, 18%, 30%, 45%, 61%, 68%, 76%, 81%) to determine the water content that provides appropriate mechanical strengths and curing times for the hydrogels, as measured using the TA Instruments Discovery Hybrid Rheometer Mark 2 using the UV oscillatory rheology measurement described in section 2.3.3.

2.3.4 - Swelling Measurements

Precursor solutions cast in 5/8'' pre-punched wells in a 1/4" thick silicone sheet placed on top of another silicone sheet to enable the gels to be easily lifted off the support following photopolymerization. Gelation was conducted using a Con-Trol-Cure Cure Zone 2 UV Flood Curing System equipped with a 400 W metal halide light source and irradiated for 20 minutes. Gels were equilibrated overnight in 100% humidity, after which they were loaded into modified 40 µm nylon cell culture inserts in which the plastic tab was cut off to allow the inserts to sit flush when placed in a 6-well plate filled with 12 mL of 0.01 M PBS. Gravimetric swelling and degradation measurements were conducted using a Mettler-Toledo MS105 Semi-Micro Balance every 15 minutes for the first hour, every 30 minutes for the next 2 hours, every hour for the next 6 hours, and then once daily until the end of the test. Wells were topped up to 12 mL of 0.01 M PBS solution keep gels completely submerged in PBS throughout the experiment. All swelling measurements were done in triplicate

using three separate gels of the same formulation, each consisting of unD-SNPs at concentrations between 0.1-10%w/v; error bars represent the standard deviation of these replicate tests.

2.3.5 - Degradation Studies

2.3.5.1 - Starch-Iodine Complexation Assay for Microplate Quantification of Starch Nanoparticles

This method for starch quantification was adapted from the protocol miniaturized by Xiao et al.[82] Calibrant standards of SNP solutions were made by serial dilution (5 mg/mL, 2.5 mg/mL, 1.25 mg/mL, 0.625 mg/mL, 0.313 mg/mL, 0.156 mg/mL) using a stock solution of 10 mg/mL SNPs in 0.01 M PBS. On a 96-well plate, 40 µL of the starch solutions was charged to each well, diluted with 60 µL of 0.01 M PBS buffer, and reacted with 100 µL of fresh 5 mM I_2 and 5 mM KI solution in 0.01 M PBS. In the blank row, 100 µL of blank 0.01 M PBS buffer was added to 100 µL of 5 mM I_2 and 5 mM KI solution in 0.01 M PBS. The plate was then analyzed using a Tecan Infinite M200 Plate Reader by first performing an absorbance scan over the wavelength range of 230 – 1000 nm to construct a standard curve. Each experiment was conducted in triplicate, with error bars corresponding to the standard deviation within the triplicate samples.

To test an unknown sample, 40 µL of the unknown solution was charged to each well, diluted with 60 µL of 0.01 M PBS buffer, and reacted with 100 µL of fresh 5 mM I_2 and 5 mM KI solution in 0.01 M PBS, in triplicate. The absorbance was then measured at 535 nm and correlated to a concentration using the constructed standard curve.

2.3.5.2 - Glucose-Hexokinase Assay

This method for glucose quantification was adapted from a protocol bulletin from Sigma-Aldrich. Using the included calibrant solution, a 5-point serial dilution (0.25 mg/mL, 0.13 mg/mL, 0.063 mg/mL, 0.031 mg/mL, 0.016 mg/mL) was made from the 1.0 mg/mL D-glucose standard provided in the kit. In a 96-well plate, 50 µL of the standard solutions was added to each well, diluted with 50 µL 0.01 M PBS, and then reacted with 100 µL of the reconstituted assay solution. The resulting absorbance was analyzed using a Tecan Infinite M200 Plate Reader by analyzing the absorbance

at 340 nm to construct a standard curve. Each experiment was conducted in triplicate, with error bars corresponding to the standard deviation within the triplicate samples.

To test an unknown sample, 50 µL of the unknown solution was charged to each well, diluted with 50 µL of 0.01 M PBS buffer, and reacted with 100 µL of reconstituted assay solution in 0.01 M PBS. The absorbance was then measured at 340 nm and correlated to a concentration using the constructed standard curve. Each experiment was done in triplicate.

2.3.5.3 - Degradation of Physically Entrapped Starch Nanoparticles in Ultraviolet-Cured Poly (Oligoethylene Glycol Methyl Ether Methacrylate) Hydrogels

Several methods were tried to selectively degrade the SNPs within the network.

Method 1: FITC-labelled SNPs were entrapped in UV-cured POEGMA as described in section 2.3.2.2 and exposed to HCl (0.1 M or 1.0 M) or NaOH (0.1 M or 1.0 M) to hydrolytically degrade the SNPs *in situ*. The fluorescence of the supernatant solution was monitored over time using a Perkin-Elmer Victor3v 1420 multi plate reader.

Method 2: Undialyzed SNP-entrapped hydrogels prepared as in section 2.3.2.2 were exposed to 20% trifluoroacetic acid (TFA) solution for 3 hours to hydrolytically degrade the SNPs *in situ*. A blank gel tested as a control to determine if any hydrolysis of the ester groups in the POEGMA methacrylate backbone was taking place by monitoring the creation of titratable groups using a Mandel Scientific auto-titrator.

Method 3: Enzymatic degradation of dialyzed SNPs (to avoid any potential enzyme inactivation by the crosslinker or plasticizer) was attempted using α-amylase, heating the enzyme to 75°C to perform the hydrolysis over 60 minutes followed by additional heating to 100°C for 10 minutes to subsequently inactivate the enzyme. Three strategies were employed to attempt to degrade the physically-entrapped SNPs: (1) SNPs were pre-degraded in suspension by incubating 1 wt% dialyzed SNPs with 0.1% w/w α-amylase for 1 hour at 75°C, after which hydrogels were fabricated following protocols in section 2.3.2; (2) 10 mg of α-amylase was added to the prepolymer aqueous

phase and encapsulated in the hydrogel *in situ* during photopolymerization following the method in section 2.3.2.2 (using dialyzed SNPs as the entrapped phase), after which the hydrogels were heated to 75°C for 18 hours to perform degradation; or (3) pre-formed D-SNP/POEGMA hydrogels prepared following the protocol in section 2.3.2.2 were swollen in an aqueous solution of 1 wt% α-amylase and incubated for 18 hours at 75°C.

2.3.5.4 - Methylene Blue Uptake Study

To assess the impact of the SNPs and SNP degradation on the kinetics and capacity of the uptake of a model dye, three 1% w/v dialyzed-SNP-entrapped gels (*n*=3 for each gel category) were made as described in section 2.3.2.2 and one set of POEGMA-only control samples (*n*=3) was made as described in section 2.3.2.1. One set of SNP/POEGMA hydrogels and the POEGMA-only controls were submerged in 12 mL of 0.01 M PBS at 75°C for 18 hours (baseline undegraded samples). A second set of SNP/POEGMA hydrogels was prepared in which 10 mg of α-amylase was added to the prepolymer solution and kept cold during gelation (to keep the enzyme from degrading the SNPs prematurely), after which the hydrogels were swollen in 12 mL of 0.01 M PBS at 75°C for 18 hours to activate the enzyme. A third set of SNP/POEGMA hydrogels was submerged in 12 mL of 1%w/v α-amylase in 0.01 M PBS at 75°C for 18 hours to facilitate enzymatic degradation of the SNPs.

Following the 18 hour incubation times described above, the gels were subsequently wicked of any water and re-submerged in 12 mL of a 5 mg/L methylene blue in 0.01 M PBS solution. A 200 µL aliquot was collected at every time point (every 30 minutes for the first 2 hours, every hour for the next 3 hours, then once a day) and replaced with 200 µL of fresh 5 mg/L methylene blue in 0.01 M PBS solution. The residual (unabsorbed) methylene blue concentration was then read by taking absorbance measurements at 665 nm using a Tecan Infinite M200 Plate Reader. The dye uptake capacity of the gels ($q_t = (C_tV_t - C_oV_o)/m$) was calculated based on the change in the supernatant solution concentration over time[83], with the error bars representing the standard deviations of the triplicate measurements.

2.4 - Results & Discussion

2.4.1 - Photorheology Results

2.4.1.1 - Optimizing Water Content of Ultraviolet-Cured Poly (Oligoethylene Glycol Methyl Ether Methacrylate) Hydrogels

The first parameter investigated in the development of this UV-curable POEGMA network was the optimum amount of water to incorporate into the gel directly during photopolymerization. This parameter was of particular importance to investigate first as it strongly influences the amount of SNPs that can be incorporated within the matrix and how well suspended they will be, both of which will directly impact the swelling and mechanical properties of the final gels. **Figure 2-1** shows the *in situ* photorheometry results characterizing the kinetics of mechanical changes in the hydrogel as the water content is changed.

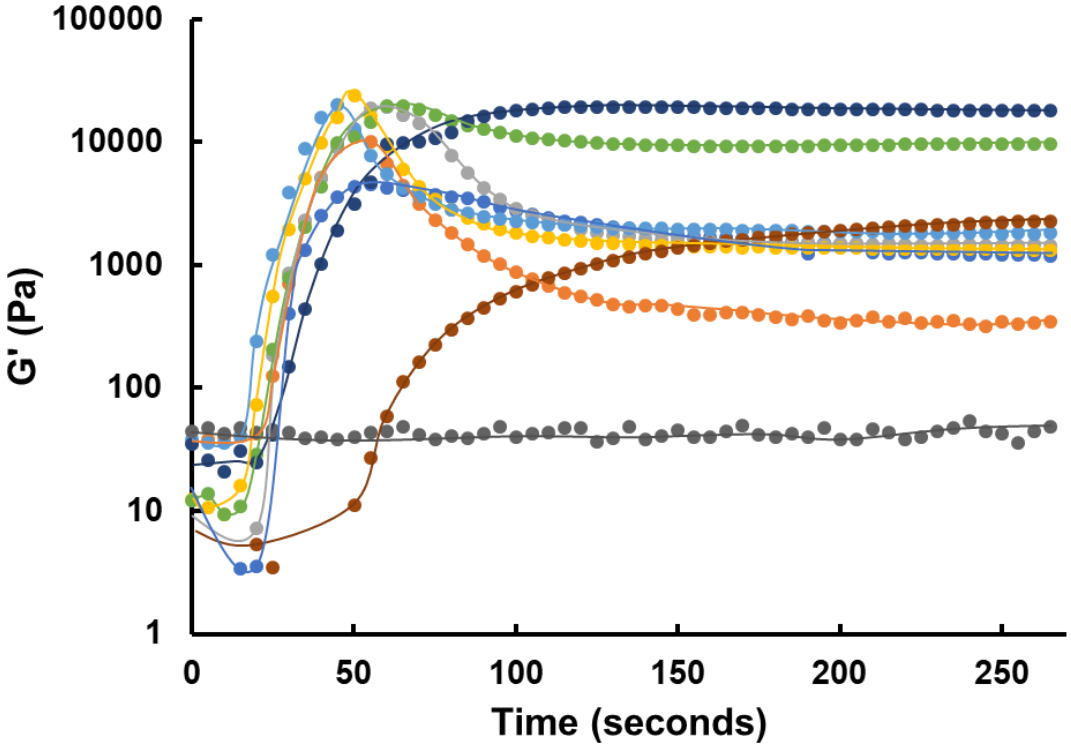

Figure 2-1. *Photorheology results for UV-PO_{50} hydrogels (no SNPs) prepared varying water content. 0% (●), 8% (●), 18% (●), 30% (●), 45% (●), 68% (●), 76% (●), 81% (●). Lines are to guide the eye.*

The neat solution of the monomers, crosslinker, and dissolved initiator creates a hydrogel with a storage modulus of ~4200 Pa within 50 seconds of irradiation. In general, adding more water allows the gelation to progress faster and produces hydrogels with an increased storage modulus,

achieving gels with G' values of up to 20,000 Pa within 120 seconds of irradiation at 68 wt% water. Further increases in water content result in the formation of weaker gels, reflecting the balance of the role of water between hydrating the growing polymer chains (favouring stiffer mechanics) but eventually diluting the polymer chains beyond their capacity to bind water (favouring weaker mechanics). As such, 68 wt% water was used for subsequent experiments.

2.4.1.2 - Ultraviolet Cured Poly (Oligoethylene Glycol Methyl Ether Methacrylate) Hydrogels with Physically Entrapped Starch Nanoparticles

The effect of adding SNPs to the aqueous phase on the mechanical properties and gelation times of the hydrogels produced is shown in **Figure 2-2**.

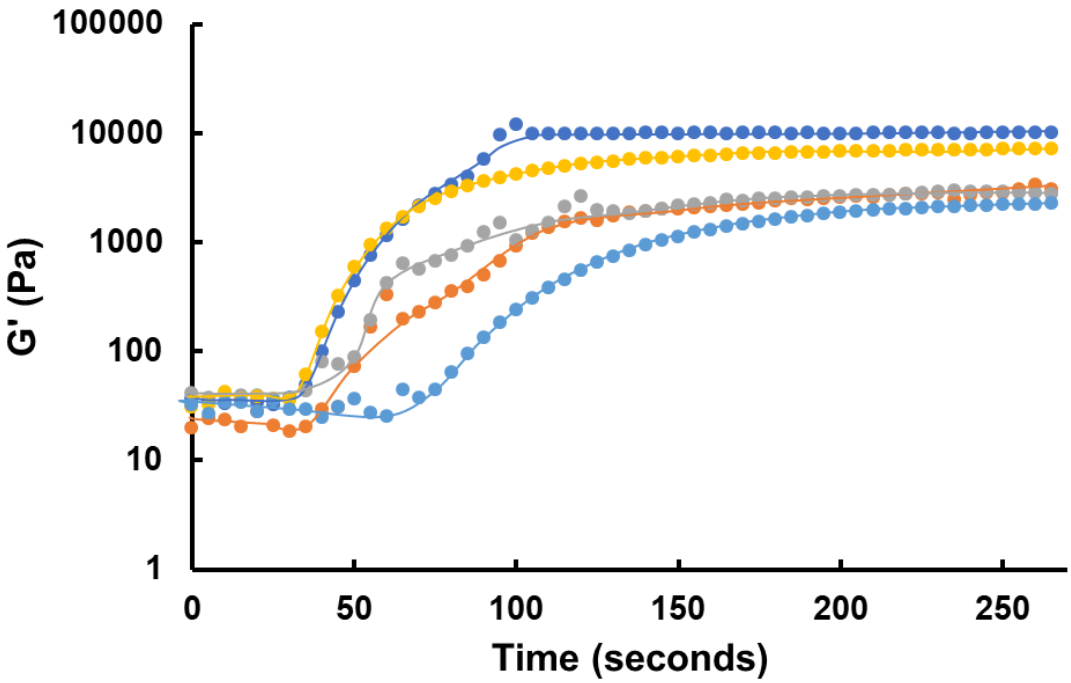

Figure 2-2. *Photorheology results for UV-PO_{50} hydrogels prepared with varying encapsulated SNP contents: 0 w/v% (Blank) (●), 0.10 w/v% unD-SNPs (●), 1.0 w/v% unD-SNPs (●), 5.0 w/v% unD-SNPs (●), 10 w/v% unD-SNPs (●). Lines are to guide the eye.*

The addition of SNPs decreases the overall mechanical strength of the gel and increases the curing time needed to achieve maximum performance; indeed, adding just 0.1%w/v SNPs decreases the mechanical strength by a factor of more than half and doubles the curing time relative to the control SNP-free hydrogel. This is consistent with the (non-interacting) SNPs disrupting network formation within the POEGMA gel phase. However, a further ten-fold increase in SNP content to 1 w/v%

shows no significant difference in either mechanics or gelation time compared to the 0.1 w/v% addition, while an additional 5-fold increase to 5 w/v% SNPs shows another substantial decrease in G' accompanied by slower gelation times. At concentrations greater than 10 w/v%, SNPs were observed to phase separate from the POEGMA precursor polymers during gelation; as such, 10 w/v% was determined to be the upper limit for SNP incorporation. Based on this data, a concentration of 1%w/v SNPs was used for subsequent entrapment studies to maintain mechanically strong gels with appreciable SNP contents while still avoiding potential phase separation challenges during polymerization.

2.4.1.3 - PO_x Series of Ultraviolet Cured Poly (Oligoethylene Glycol Methyl Ether Methacrylate) Hydrogels with Physically Entrapped Starch Nanoparticles

The effect of varying the monomer ratios of long chain $OEGMA_{500}$ and short chain $M(EO)_2MA$ on the mechanics of the nanocomposite hydrogels is shown in **Figure 2-3**.

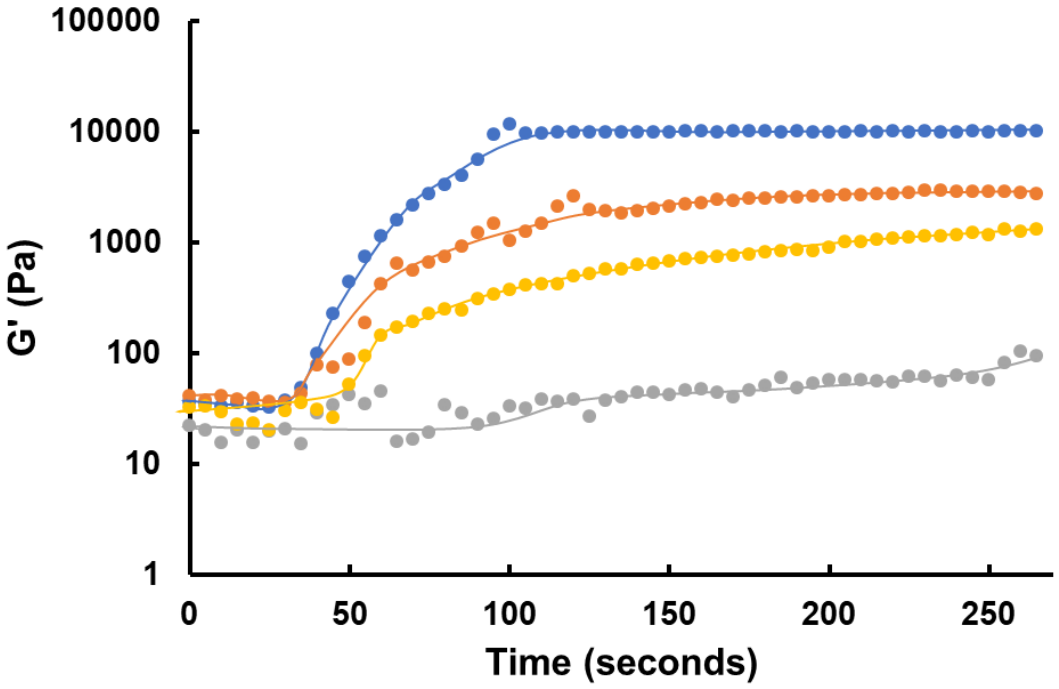

Figure 2-3. *Photorheology results for UV-PO_{50} hydrogels prepared with varying SNP concentrations and comonomer contents: 0 w/v%-PO_{50} (Blank) (●), 1.0 w/v% unD-SNPs-PO_{50} (●), 1.0 w/v% unD-SNPs-PO_0 (●), 1.0 w/v% unD-SNPs-PO_{100}(●). Lines are to guide the eye.*

The 50/50 ratio of long and short chain comonomer was demonstrated to exhibit the best mechanical properties. Using only long-chain monomer resulted in somewhat slower gelation and

weaker mechanics, consistent with the increased steric inhibition of the longer side chain on the polymerization process; using only short-chain monomer resulted in the formation of highly opaque materials that had a more phase separated texture (consistent with the formed polymer being below its phase transition temperature at room temperature[46]) and did not fill the full area between the parallel plates, resulting in poor data collection over time.

2.4.1.4 - Crosslinker Series of Ultraviolet Cured Poly (Oligoethylene Glycol Methyl Ether Methacrylate) Hydrogels with Physically Entrapped Starch Nanoparticles

The effect of changing the amount of the crosslinker EGDMA in the hydrogel recipe on resulting gel mechanics is shown in **Figure 2-4**.

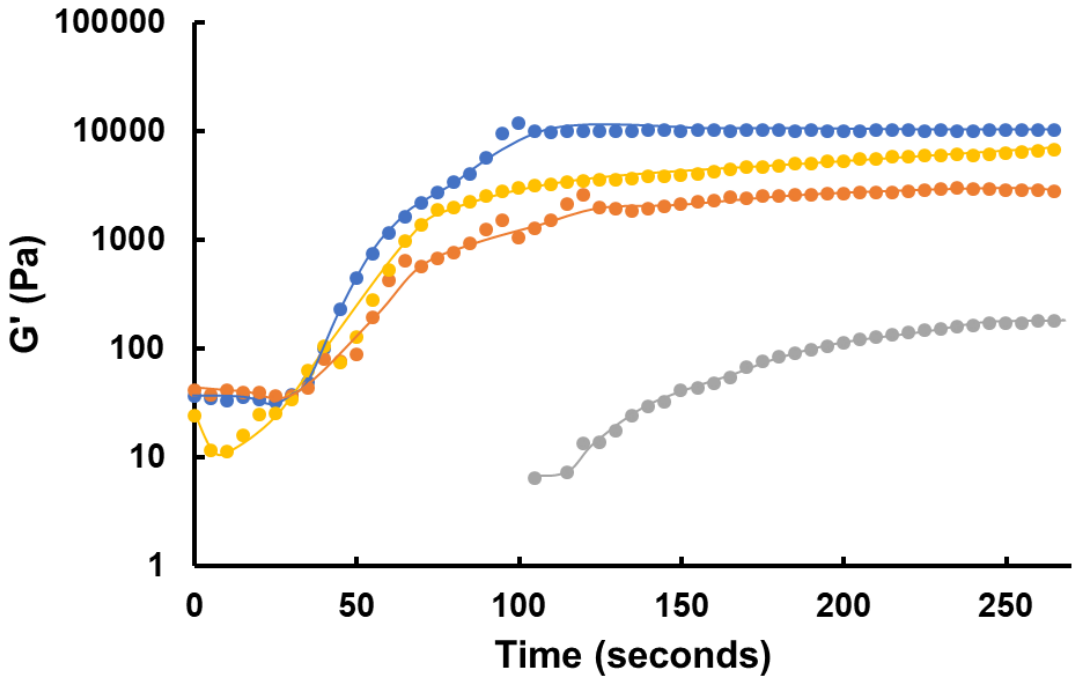

Figure 2-4. *Photorheology results for UV-PO$_{50}$ hydrogels prepared with varying crosslinker contents: 0 w/v% unD-SNP-2:1 monomer/crosslinker (Blank) (●), 1.0 w/v% unD-SNPs-2:1 monomer/crosslinker (control) (●), 1.0 w/v% unD-SNPs-4:1 monomer/crosslinker (●), 1.0 w/v% unD-SNPs-1:1 monomer/crosslinker (●). Lines are to guide the eye.*

As expected, as the amount of crosslinker is increased, stiffer and faster curing hydrogels are produced. Of note, the 1:1 molar ratio of monomer to crosslinker SNP-encapsulated hydrogel shows the same storage modulus as the 2:1 molar ratio POEGMA-only hydrogel, such that the amount of crosslinker used can compensate for the weaker mechanics that result from SNP incorporation.

2.4.2 - Swelling Kinetics

2.4.2.1 - Ultraviolet Cured Poly (Oligoethylene Glycol Methyl Ether Methacrylate) Hydrogels with Physically Entrapped Starch Nanoparticles

The swelling response of hydrogels formed with different concentrations of SNPs in 0.01 M PBS is shown in **Figure 2-5**.

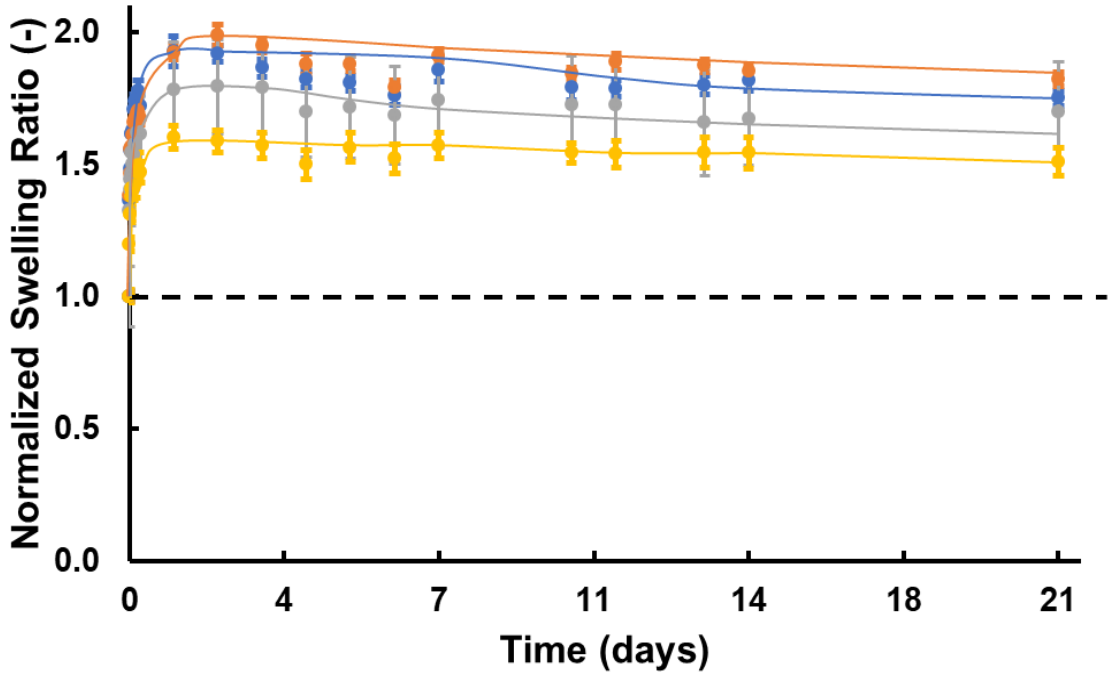

Figure 2-5. *Normalized swelling kinetics for UV- PO_{50} hydrogels prepared with varying SNP contents: 0 w/v% unD-SNP (Blank) (●), 0.10 w/v% unD-SNPs (●), 1.0 w/v% unD-SNPs (●), 10 w/v% unD-SNPs (●). Lines are a guide to the eye.*

Each gel tested equilibrates over the first 24 hours of swelling and exhibits no significant subsequent change in swelling (due to degradation or other impacts) over the full 3-week study period. Overall, the swelling ratio increases upon the incorporation of a small fraction of SNPs but, as higher SNP concentrations are added, the swelling ratio decreases. We hypothesize this result is related to the pre-swollen nature of the SNPs during the *in situ* polymerization process; as the volume fraction of SNPs increases, the pre-swollen SNPs account for more of the total gel volume and less overall swelling is observed in the gel as a whole.

2.4.2.2 - PO_x Series of Ultraviolet Cured Poly (Oligoethylene Glycol Methyl Ether Methacrylate) Hydrogels with Physically Entrapped Starch Nanoparticles

The effect of the long:short chain monomer ratio used to prepare the UV-POEGMA-SNP gels on the swelling capacity of the hydrogels is shown in **Figure 2-6**.

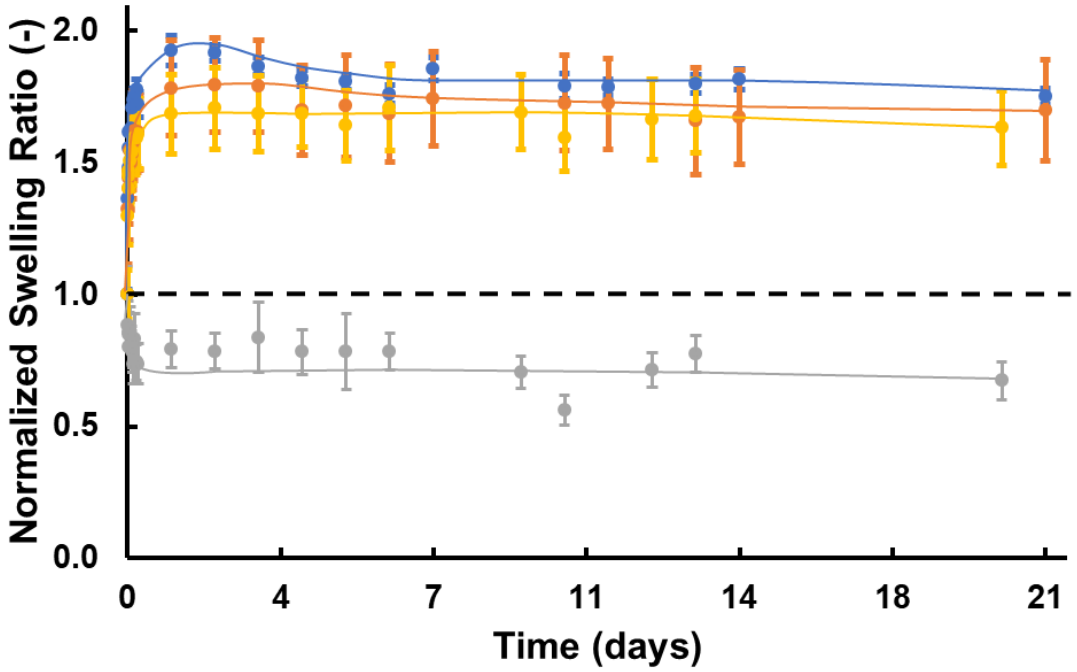

Figure 2-6. *Normalized swelling kinetics for UV-PO_{50}-unD-SNP hydrogels prepared with varying comonomer content. 0 w/v% unD-SNP-PO_{50} (Blank) (●), 1.0 w/v% unD-SNPs-PO_{50} (●), 1.0 w/v% unD-SNPs-PO_0 (●), 1.0 w/v% unD-SNPs-PO_{100} (●). Lines are a guide to the eye.*

Both the 50/50 mixture of long:short chain monomers and the all-long chain monomer gel exhibited similar swelling responses, equilibrating within 24 hours to between 1.5-2 times its initial weight. In contrast, the all-short chain monomer gel de-swelled over time, consistent with its volume phase transition temperature lying below room temperature that was used for swelling testing. Of note, the still substantial swelling response observed for the 50/50 gel contrasts what was observed in the absence of SNPs, in which the 50:50 gel did not swell or deswell significantly over time. This result suggests that the SNPs can alter the swelling response of the POEGMA gel even at relatively low vol%, provided that the bulk gel phase does itself undergo a phase transition.

2.4.2.3 - Crosslinker Series of Ultraviolet Cured Poly (Oligoethylene Glycol Methyl Ether Methacrylate) Hydrogels with Physically Entrapped Starch Nanoparticles

The effect of varying the EGDMA crosslinker amount on gel swelling is shown in **Figure 2-7**.

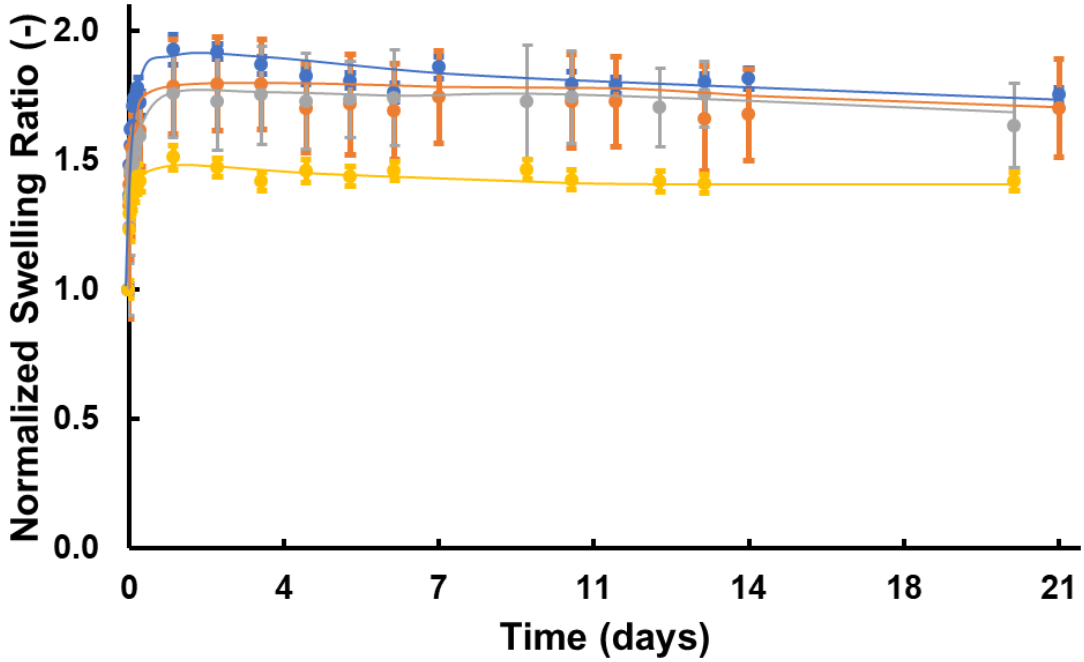

Figure 2-7. *Normalized swelling kinetics for UV- PO_{50} hydrogels prepared with varying equivalents of EGDMA crosslinker. 0.0 w/v% unD-SNP-2:1 monomer/crosslinker (Blank) (●), 1.0 w/v% unD-SNPs-2:1 monomer/crosslinker (●), 1.0 w/v% unD-SNPs-4:1 monomer/crosslinker (●), 1.0 w/v% unD-SNPs-1:1 monomer/crosslinker (●). Lines are a guide to the eye.*

No significant difference was observed in the kinetics or equilibrium swelling responses of the 4:1 and 1:1 monomer to crosslinker ratios on SNP-POEGMA hydrogels, with both swelling to ~1.75 times their initial weight; this degree of swelling is similar to that observed for the no-SNP control POEGMA hydrogel. The similarity between these results is somewhat surprising but can be related to the role of SNPs in interrupting the continuous POEGMA network structure and thus reducing the differences observed between different EGDMA content hydrogels. Increasing the crosslinker to 2x the base recipe results in lower swelling (~1.5-fold swelling). However, the differences in swelling between the samples are relatively small compared to the observed differences in the overall mechanics of the different hydrogels (Fig. 2-4), again suggesting that the presence of SNPs normalizes the expected swelling responses relative to what would be observed with the POEGMA gels themselves.

2.4.3 - Degradation of Starch Nanoparticles

2.4.3.1 - Starch-Iodine Complexation Assay for Microplate Quantification of Starch Nanoparticles

Before assessing the potential for SNP degradation *in situ* inside the hydrogels, methods were established to measure both free starch and glucose, the latter of which is the full degradation product of SNPs. First, a starch-iodine assay was performed that is based on the ability of starch to chelate to I_3^- and thus create a deep purple complex which can be detected at 530-580 nm depending on the source of starch. To identify the maximum absorbance of the different SNPs used in this work, an absorbance scan was done to find the optimal wavelength for detection, as shown in **Figure 2-8A**.

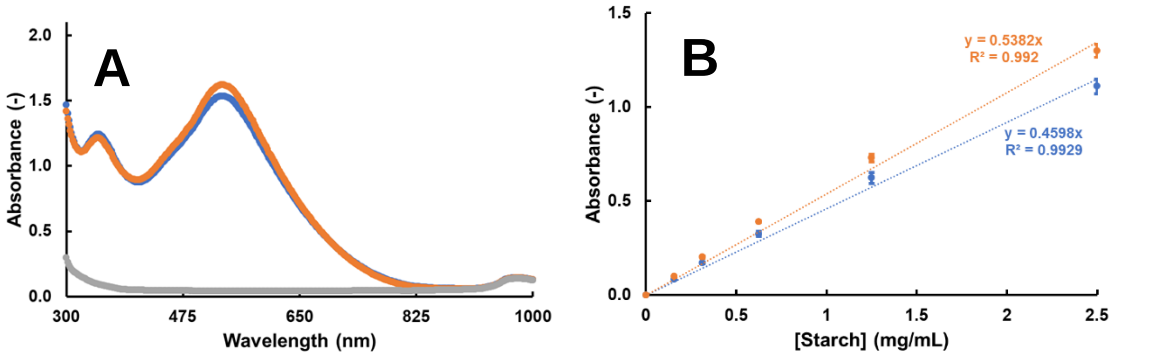

Figure 2-8. *Starch-iodine assay calibration:* **A.** *Absorbance scan of undialyzed SNPs (Blank) (●), dialyzed SNPs (●), and predegraded aldehyde SNPs (●) following assay treatment;* **B.** *Calibration curves for the starch-iodine assay for undialyzed SNPs (●) and dialyzed SNPs (●).*

Undialyzed and dialyzed SNPs all showed a maximum absorbance at 535 nm, leading to linear calibration curves of absorbance versus SNP concentration that were very similar (**Figure 2-8B**). However, the predegraded (aldehyde functionalized) SNPs did not complex with iodine to produce a colored complex, as illustrated by the grey line in **Figure 2-8A**. The lack of complexation is most likely attributable to the periodate oxidation process, which breaks apart the vicinal diols in the glucose monomers of starch that are important for starch to effectively interact with the I_3^- and form the coloured complex. Hence, no result could be read from the starch-iodine assay for any potential degradation of the pre-degraded SNP samples upon enzyme or acid treatment.

2.4.3.2 - Glucose-Hexokinase Assay

The hexokinase glucose assay enables glucose detection by reacting glucose with the catalytic enzyme hexokinase, which phosphorylates the glucose molecule at the C6 position by converting a molecule of adenosine triphosphate (ATP) to adenosine diphosphate (ADP). The glucose-6-phospate (G6P) molecule is then oxidized to 6-phosphogluconate by reducing nicotinamide adenine dinucleotide (NAD^+) to NADH, again enzymatically catalyzed by using glucose-6-phosphate dehydrogenase. The subsequent increase in absorbance at 340 nm can be used to quantify the glucose concentration. The absorbance scan shown in **Figure 2-9A** confirms the wavelength of detection at 340 nm and no absorbance from the blank solutions. A calibration curve constructed from these scans is shown in **Figure 2-9B**, providing a good linear fit up to a glucose concentration of 0.25 mg/mL. This assay was chosen as it has a different analysis wavelength compared to the previously described starch-iodine assay whereas the standard glucose-horsereadish peroxidase assay would have had the same absorbance wavelength.

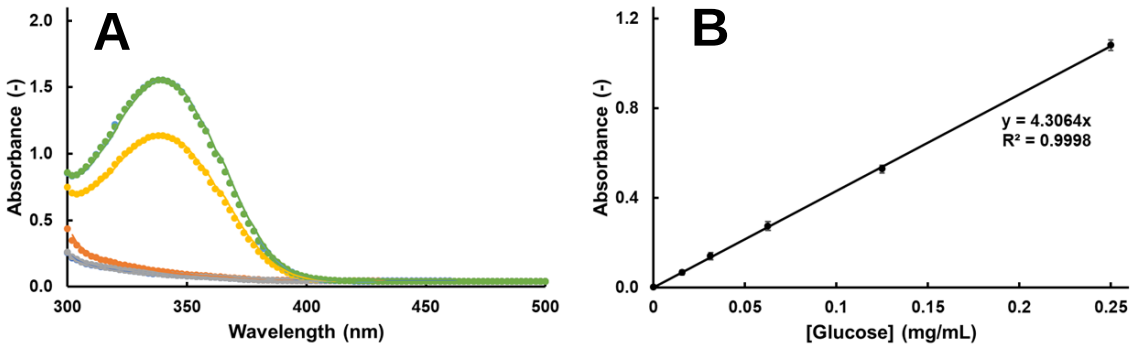

Figure 2-9. *Glucose-hexokinase assay:* **A.** *Absorbance scan of 0.01 M PBS (Blank) (●), D-glucose (Blank) (●), Assay Reagent (Blank) (●), 0.25mg/mL D-glucose (●), 0.50 mg/mL D-glucose (●), 1.0 mg/mL D-glucose (●);* **B.** *Calibration curve for the glucose-hexokinase assay.*

2.4.3.3 - Enzymatic Degradation of Physically Entrapped Starch Nanoparticles in Ultraviolet-Cured Poly (Oligoethylene Glycol Methyl Ether Methacrylate) Hydrogels using α-Amylase

Using both the glucose-hexokinase assay to detect glucose degradation products and the starch-iodine assay to quantify released starch in the media surrounding the gels, a profile of degradation

products can be established for different methods of erosion of the impregnated SNPs. **Figure 2-10** shows the impact of α-amylase degradation on the entrapped SNP component of the hydrogels.

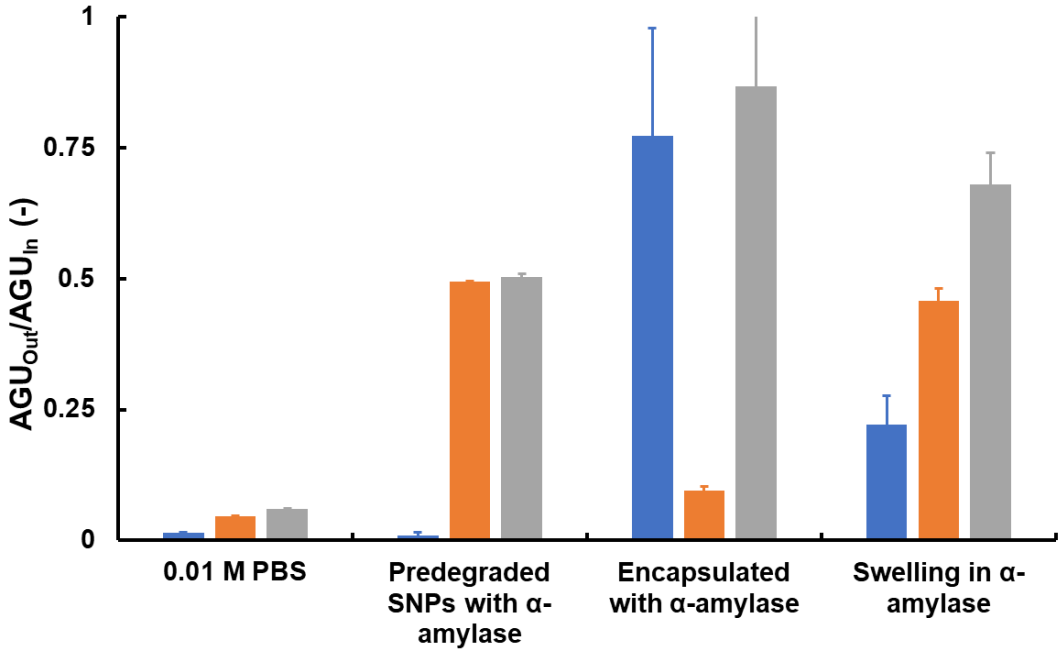

Figure 2-10. *Summary of α-amylase efficacy on SNP degradation. Anhydrous glucose unit (AGU) Ratio AGU $_{Out}$/AGU $_{In}$ for starch (●), glucose (●) and total (●).*

Clear differences were observed in the effectiveness of each method. Significantly more glucose release was observed via amylase degradation of pre-degraded SNPs or by post-swelling the hydrogel with entrapped non-degraded SNPs in an amylase solution, with 46±2% and 49±0.1% respectively of the starch initially loaded into the hydrogels being degraded into glucose units and removed from the hydrogel. In contrast, encapsulated amylase results in the conversion of relatively little starch to glucose, suggesting at least partial deactivation of the enzyme during the photopolymerization process. undegraded control results in low signals before and after treatment, confirming the specificity of the signal to degraded SNPs.

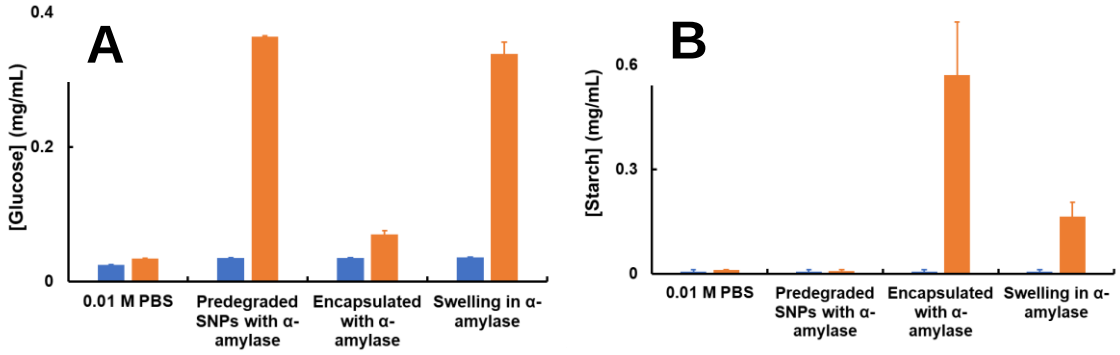

Figure 2-11. *Degradation of SNPs using α-amylase* **A.** *Glucose concentration in solution surrounding the hydrogel (as per the glucose-hexokinase assay) following different methods of enzymatic degradation of SNPs using α-amylase before degradation event (●) and after degradation event (●).* **B.** *Starch concentration in solution surrounding the hydrogel (as per the starch-iodine assay) after different methods of enzymatic degradation of SNPs using α-amylase*

By analyzing the results of the starch-iodine assay in **Figure 2-11B**, the amount of macromolecular starch released from the hydrogel as a result of the degradation process can also be estimated. In this case, swelling in amylase solution resulted in 22±5% of the original glucose units present in the hydrogel being released into the supernatant after degradation; combining this amount with the estimated glucose release in **Figure 2-12**, 68±6% of the total SNPs added to the hydrogels are degraded upon incubation in the amylase solution. Interestingly, however, the encapsulated amylase produced a significantly higher amount of starch by-product, with 77±20% of the original number of glucose units in the hydrogel detected in the supernatant in the form of released starch. This suggests that the encapsulated enzyme is at least partially active and capable of degrading the SNPs *in situ*, although the product is oligomeric starch rather than monomeric glucose. As such, we hypothesize that the improved distribution of enzyme throughout the hydrogel in the encapsulated samples results in improved overall removal of the starch from the network, just in a primarily macromolecular rather than monomeric form due to the anticipated lower activity of the encapsulated enzyme. Similarly, when pre-treating the SNPs with amylase, the data suggests that while substantial glucose by-products are produced during the pre-degradation step (outside the gel), the residual SNPs inside the gel either do not further degrade or degrade into macromolecular starch that is hard to remove from the network. As such, while the products of the degradation are

different depending on the pathway used, the use of amylase can degrade the large majority of entrapped SNPs inside the hydrogel.

Hydrolytic degradation was also attempted using various acids (1.0 M and 0.1 M HCl and bases (1.0 M and 0.1 M NaOH) using SNP-FITC and directly treating the hydrogels to these solutions, as shown in **Appendix 1**. When using 20% TFA for hydrolytic degradation, it was observed that only 10% of the total starch inside the initial hydrogel was detected in the supernatant solution. By using blanks of POEGMA-only hydrogels, conductometric titrations confirmed that that no new acid groups form in the polymer matrix alone from ester hydrolysis of the POEGMA backbone (**Appendix 2**), such that the TFA could specifically degrade the *in situ*-loaded SNPs. However, given biological tolerability of TFA as a degradation agent relative to amylase and the much lower efficacy of TFA-based degradation of the SNPs, no further work was conducted on this strategy.

2.4.3.4 - Methylene Blue Uptake Results

To assess the differences in internal porosity generated within the hydrogels as a result of the degradation of the *in situ*-loaded SNPs, a methylene blue sorption assay was conducted. An absorbance scan of methylene blue is shown in **Figure 2-12A**, showing a maximum absorbance at 665 nm that could be used to construct a linear calibration curve (**Figure 2-12B**). In a methylene blue uptake experiment, hydrogels before and after SNP degradation were incubated in a methylene blue solution for fixed periods of time and the residual absorbance in the

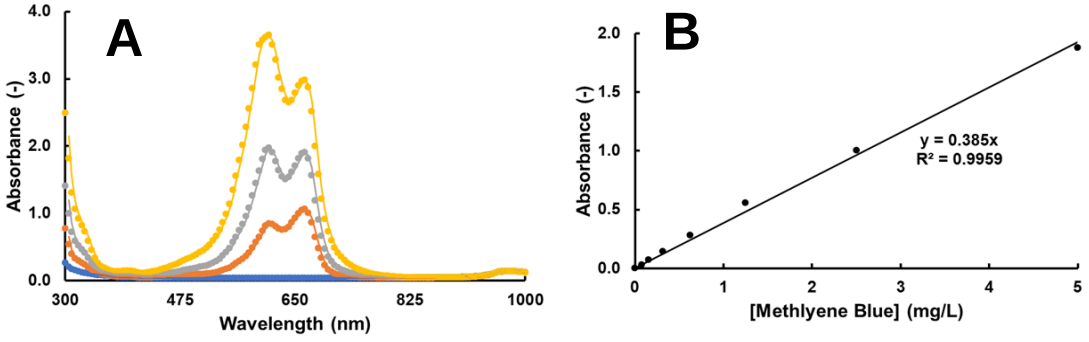

Figure 2-12. *Methylene blue assay calibration:* **A.** *Absorbance scan of methylene blue. 0.01 M PBS (Blank) (●), 2.5 mg/L methylene blue in 0.01 M PBS (●), 5.0 mg/L methylene blue in 0.01 M PBS (●), 10 mg/L methylene blue in 0.01 M PBS (●). Lines are a guide for the eye.* **B.** *Calibration curve for methylene blue.*

solution (i.e. the fraction of methylene blue not taken up into the hydrogel) was measured using the same protocol used for the controls. The result was subsequently converted to an uptake capacity of the gel by dividing the mass of methylene blue taken up into the gel by the dry mass of the gel components (q_t), the results of which are shown in **Figure 2-13**.

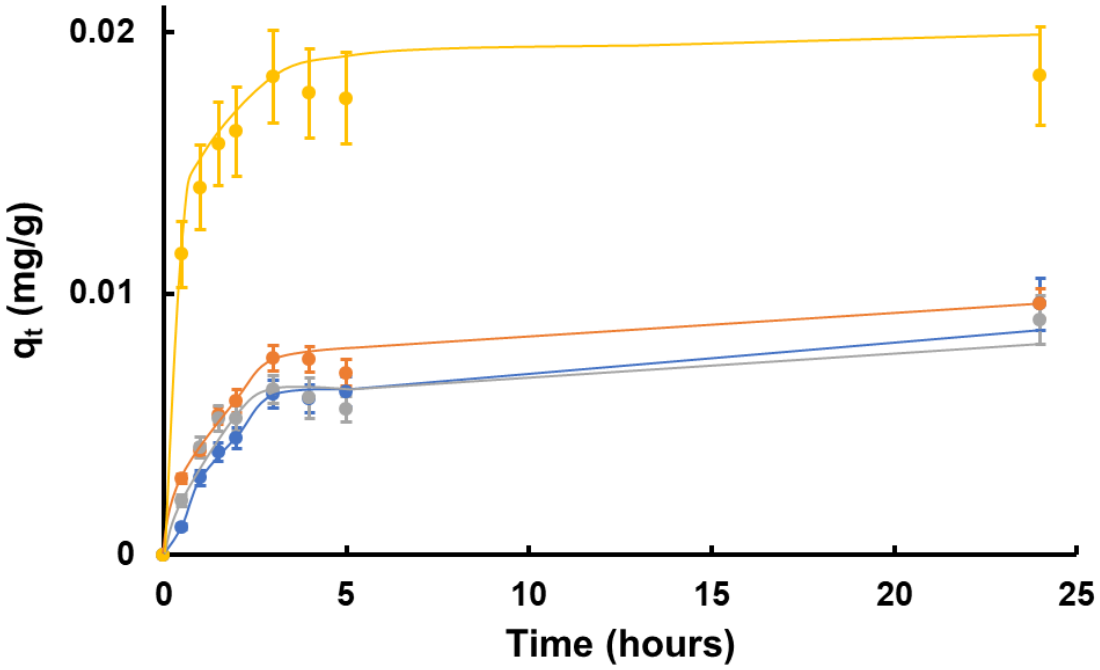

Figure 2-13. *Methylene blue uptake ratio (q_t) of SNP-POEGMA hydrogels before and after degradation: $UVPO_{50}$-0%- D-SNP swollen in 0.01 M PBS for 18 hours (no SNP blank) (●); $UVPO_{50}$-1.0%- D-SNP swollen in 0.01 M PBS for 18 hours (SNP blank). (●), $UVPO_{50}$-1.0%- D-SNP + 10 mg α-amylase swollen in 0.01 M PBS for 18 hours (encapsulated amylase). (●), $UVPO_{50}$-1.0%- D-SNP swollen in 1%w/v α-amylase in 0.01 M PBS for 18 hours. (●). Lines are a guide for the eye.*

The gel exposed to 1%w/v α-amylase solution both uptakes the methylene blue faster as well as exhibits a much higher total uptake capacity for methylene blue. This condition is also the condition noted to result in the most glucose production upon enzymatic degradation (**Figure 2-11**), suggesting that the pores templated by the SNPs during the polymerization process are now free volume that both accelerate diffusion into the hydrogel as well as provide increasing adsorption/absorption sites for methylene blue uptake. In addition, the in-diffusion of amylase into the hydrogels in this case is more likely to create clear pathways of degraded starch templated

pores for the methylene blue to access on the timescale of this uptake experiment. In contrast, the encapsulated-only amylase sample does not show a significantly increased uptake rate or capacity relative to the pre-degraded controls, consistent with the dominant production of oligomeric starch (a portion of is still present and filling the SNP-templated pore volumes) rather than glucose (which can freely move out of the gel) and the lower probability of creating pores accessible to the surface for fast in-diffusion of methylene blue.

2.5 - Chapter Summary & Conclusions

2.5.1 - Conclusions

A photopolymerized UV initiated hydrogel system based on OEGMA was demonstrated to physically entrap up to 10 w/v% SNPs to form a nanocomposite hydrogel structure. The physical parameters of these subsequent gels were investigated, including the effects of SNP concentration, monomer ratio, and crosslinker amount on the curing kinetics, storage modulus and swelling of the hydrogels produced. While a range of different properties can be achieved, the use of a 50/50 long/short chain monomer ratio with 1.0 w/v% SNPs and a 1:1 mono:difunctional monomer ratio ($UVPO_{50}$-1.00w/v%-unD-SNP) yielded a particularly interesting gel with a G' of 3000 Pa formed within 165 seconds of photopolymerization. Using this gel, it was demonstrated that dialyzed SNPs can be degraded selectively *in situ* inside the gel using α-amylase. Assays for the degradation products of both oligomeric starch and monomeric glucose in the supernatant around the gels indicated up to ~77% degradation of the total amount of starch initially present in the hydrogels in the form of entrapped SNPs, with post-incubation in an amylase solution creating more glucose by-products while encapsulated amylase enzyme resulted in more macromolecular starch-based by-products. The generation of additional porosity inside the gel as a result of this SNP degradation process was confirmed by the faster and higher equilibrium sorption capacity of amylase-incubated gels for methylene blue compared to gels not exposed to degradation conditions. In the context of hydrogel materials, this capacity to generate pores inside hydrogels on the length scale of SNP diameter (~20-50 nm) using an enzymatic degradation approach that does not leave behind any

toxic by-products may be of significant interest for a variety of biomedical applications in which improved transport into bulk hydrogels may be desirable (e.g. tissue engineering, accelerated drug delivery, etc.).

2.5.2 - Summary

- An ultraviolet curable POEGMA hydrogel can be fabricated using various ratios of $OEGMA_{500}$, $M(EO)_2MA$ as the monomers, EGDMA as the crosslinker, and Irgacure 2959 as the free radical initiator.
- SNPs can be incorporated in these gels at up to 10%w/v, albeit with trade-offs such as decreases in mechanical performance and increases in curing time at higher SNP contents.
- UV-POEGMA-SNP gels can be designed with storage moduli of up to 10 kPa, curing times within 240 seconds, and swelling responses of up to twice their initial weight in 0.01 M PBS.
- The entrapped SNPs can be partially degraded hydrolytically (up to ~10% of the initial mass of SNPs), or (preferentially) enzymatically using α-amylase. Encapsulating amylase in the gels is the most effective enzymatic method for SNP degradation, enabling up to a >87% removal of SNPs as per starch and glucose detection assays. However, post-treatment with amylase solution results in the generation of significantly more monomeric (and likely also short oligomeric) glucose while encapsulation results in the generation of primarily macromolecular starch by-products.
- The resulting nanoporosity generated can facilitate significantly faster and higher capacity uptake of a model dye (methylene blue).
- The resulting nanoporous hydrogels may have applications in bioseparations or drug delivery applications in which the generation of larger but still nanoscale pores inside a hydrogel may be relevant for various transport-related applications.

2.6 - References

1. Agrawal, S. K.; Sanabria-DeLong, N.; Tew, G. N.; Bhatia, S. R., Nanoparticle-Reinforced Associative Network Hydrogels. *Langmuir* **2008,** *24* (22), 13148-13154.
2. Jamshidian, M.; Tehrany, E. A.; Imran, M.; Jacquot, M.; Desobry, S., Poly-Lactic Acid: Production, Applications, Nanocomposites, and Release Studies. *Comprehensive Reviews in Food Science and Food Safety* **2010,** *9* (5), 552-571.
3. Bel Haaj, S.; Thielemans, W.; Magnin, A.; Boufi, S., Starch nanocrystals and starch nanoparticles from waxy maize as nanoreinforcement: A comparative study. *Carbohydr. Polym.* **2016,** *143*, 310-7.
4. Smeets, N. M.; Bakaic, E.; Patenaude, M.; Hoare, T., Injectable poly(oligoethylene glycol methacrylate)-based hydrogels with tunable phase transition behaviours: physicochemical and biological responses. *Acta Biomater.* **2014,** *10* (10), 4143-55.
5. Bakaic, E.; Smeets, N. M. B.; Dorrington, H.; Hoare, T., "Off-the-shelf" thermoresponsive hydrogel design: tuning hydrogel properties by mixing precursor polymers with different lower-critical solution temperatures. *RSC Advances* **2015,** *5* (42), 33364-33376.
6. Bakaic, E.; Smeets, N. M. B.; Hoare, T., Injectable hydrogels based on poly(ethylene glycol) and derivatives as functional biomaterials. *Rsc Advances* **2015,** *5* (45), 35469-35486.
7. De France, K. J.; Chan, K. J.; Cranston, E. D.; Hoare, T., Enhanced Mechanical Properties in Cellulose Nanocrystal-Poly(oligoethylene glycol methacrylate) Injectable Nanocomposite Hydrogels through Control of Physical and Chemical Cross-Linking. *Biomacromolecules* **2016,** *17* (2), 649-60.
8. Sivakumaran, D.; Maitland, D.; Hoare, T., Injectable microgel-hydrogel composites for prolonged small-molecule drug delivery. *Biomacromolecules* **2011,** *12* (11), 4112-20.
9. Broguiere, N.; Husch, A.; Palazzolo, G.; Bradke, F.; Madduri, S.; Zenobi-Wong, M., Macroporous hydrogels derived from aqueous dynamic phase separation. *Biomaterials* **2019,** *200*, 56-65.
10. Huebsch, N.; Lippens, E.; Lee, K.; Mehta, M.; Koshy, S. T.; Darnell, M. C.; Desai, R. M.; Madl, C. M.; Xu, M.; Zhao, X.; Chaudhuri, O.; Verbeke, C.; Kim, W. S.; Alim, K.; Mammoto, A.; Ingber, D. E.; Duda, G. N.; Mooney, D. J., Matrix elasticity of void-forming hydrogels controls transplanted-stem-cell-mediated bone formation. *Nat Mater* **2015,** *14* (12), 1269-77.
11. Mooney, N. D. H. C. M. M. K. L. M. M. X. D. J. Injectable, Pore-Forming Hydrogels For Materials-Based Cell Therapies. 2014.
12. Gomes, R. F.; de Azevedo, A. C.; Pereira, A. G.; Muniz, E. C.; Fajardo, A. R.; Rodrigues, F. H., Fast dye removal from water by starch-based nanocomposites. *J. Colloid Interface Sci.* **2015,** *454*, 200-9.
13. Deborah Le Corre, J. B., and Alain Dufresne, Starch Nanoparticles: A Review. *Biomacromolecules* **2010,** *11* (5), 15.
14. Chiu, C.; Solarek, D., Modification of Starches. In *Starch: Chemistry and Technology*, Third Edition ed.; Elsevier inc.: 2009; p 27.
15. Moad, G., Chemical modification of starch by reactive extrusion. *Prog. Polym. Sci.* **2011,** *36* (2), 218-237.
16. Chakraborty, S.; Sahoo, B.; Teraoka, I.; Gross, R. A., Solution properties of starch nanoparticles in water and DMSO as studied by dynamic light scattering. *Carbohydr. Polym.* **2005,** *60* (4), 475-481.
17. Avval, M. E.; Moghaddam, P. N.; Fareghi, A. R., Modification of starch by graft copolymerization: A drug delivery system tested for cephalexin antibiotic. *Starch-Starke* **2013,** *65* (7-8), 572-583.
18. Namazi, H.; Dadkhah, A., Surface modification of starch nanocrystals through ring-opening polymerization of ε-caprolactone and investigation of their microstructures. *J. Appl. Polym. Sci.* **2008,** *110* (4), 2405-2412.

19. Ptaszek, A.; Lukasiewicz, M.; Bednarz, S., Environmental friendly polysaccharide modification - rheological properties of oxidized starches water systems. *Starch-Starke* **2013,** *65* (1-2), 134-145.
20. Jones, N. A.; Chang, S. R.; Troske, W. J.; Clarkson, B. H.; Lahann, J., Nanoparticle-Based Targeting and Detection of Microcavities. *Adv Healthc Mater* **2017,** *6* (1).
21. Araujo, M. A.; Cunha, A. M.; Mota, M., Changes in morphology of starch-based prothestic thermoplastic material during enzymatic degradation. *J. Biomater. Sci. Polym. Ed.* **2004,** *15* (10), 1263-80.
22. Azevedo, H. S.; Reis, R. L., Encapsulation of alpha-amylase into starch-based biomaterials: an enzymatic approach to tailor their degradation rate. *Acta Biomater.* **2009,** *5* (8), 3021-30.
23. G. Ongen, G. Y., R.O.J. Jongboom, H. Feil, Encapsulation of a-amylase in a starch matrix. *Carbohydr. Polym.* **2002,** *50*, 5.
24. Hermanson, G. T., *Bioconjugate Techniques*. 3rd ed.; Elsevier Inc.: 2013.
25. Maia, J.; Carvalho, R. A.; Coelho, J. F. J.; Simoes, P. N.; Gil, M. H., Insight on the periodate oxidation of dextran and its structural vicissitudes. *Polymer* **2011,** *52* (2), 258-265.
26. Maia, J.; Ferreira, L.; Carvalho, R.; Ramos, M. A.; Gil, M. H., Synthesis and characterization of new injectable and degradable dextran-based hydrogels. *Polymer* **2005,** *46* (23), 9604-9614.
27. Khoushabi, A.; Schmocker, A.; Pioletti, D. P.; Moser, C.; Schizas, C.; Manson, J. A.; Bourban, P. E., Photo-polymerization, swelling and mechanical properties of cellulose fibre reinforced poly(ethylene glycol) hydrogels. *Compos. Sci. Technol.* **2015,** *119*, 93-99.
28. Schmocker, A.; Khoushabi, A.; Frauchiger, D. A.; Gantenbein, B.; Schizas, C.; Moser, C.; Bourban, P. E.; Pioletti, D. P., A photopolymerized composite hydrogel and surgical implanting tool for a nucleus pulposus replacement. *Biomaterials* **2016,** *88*, 110-9.
29. Wax, A.; Backman, V.; Schmocker, A. M.; Khoushabi, A.; Gantenbein-Ritter, B.; Chan, S.; Bonél, H. M.; Bourban, P.-E.; Månson, J. A.; Schizas, C.; Pioletti, D.; Moser, C., Minimally invasive photopolymerization in intervertebral disc tissue cavities. In *Biomedical Applications of Light Scattering VIII*, 2014.
30. Xiao, Z.; Storms, R.; Tsang, A., A quantitative starch–iodine method for measuring alpha-amylase and glucoamylase activities. *Anal. Biochem.* **2006,** *351* (1), 3.
31. Zhou, C.; Wu, Q.; Lei, T.; Negulescu, I. I., Adsorption kinetic and equilibrium studies for methylene blue dye by partially hydrolyzed polyacrylamide/cellulose nanocrystal nanocomposite hydrogels. *Chem. Eng. J.* **2014,** *251*, 17-24.

3 Methacrylate-Functionalized Starch Nanoparticle Mediated Crosslinking of Ultraviolet-Cured Poly (Oligoethylene Glycol Methyl Ether Methacrylate) Hydrogels

3.1 - Introduction & Objectives

In Chapter 2, starch nanoparticles were used as physical fillers for hydrogels but were not covalently attached to the surrounding hydrogel network. However, the use of nanoparticles, and particularly degradable nanoparticles, as crosslinkers for hydrogels is itself an area of significant interest and promise. Such a hydrogel would have macroscopic properties that are more directly related to the integration of the nanoparticles into the network structure, instead of having primarily an additive effect as a suspended phase. In this context, the degradability, swelling, and (in some cases) thermoresponsiveness elicited from the nano component can be more directly controlled by the incorporated nanophase.[8]

Many soft nanogels have been described and studied, deriving from both synthetic polymers such as poly (vinyl alcohol) or poly(ethylene oxide) and natural polymers such as starch, chitosan and alginates.[10, 84-86] In one such example, starch microspheres were readily made by using sodium trimetaphosphate (STMP) to crosslink the starch. These structures were than used as the aqueous phase in a water/oil emulsion to create microspheres, emulsified as the crosslinking of starch is taking place. The resultant microspheres were tested for their efficacity of drug delivery with methylene blue as a model drug, showing an initial burst release followed by sustained release over time.[87]

Nanoparticles can be used to form hydrogel networks in different ways. If the building block is a nanogel that itself swells in water, the nanoparticles can themselves be building blocks of a hydrogel

network. The interactions between microgels holding the network together are in some cases physical; as an example, Hu et al. showed that poly (N-isopropylacrylamide-co-acrylic acid) microgels could self-aggregate into a solid opaque hydrogel upon heating to 37°C that could facilitate sustained release of a model macromolecular therapeutic (fluorescein-labeled dextran) over several weeks.[85, 88] In other cases, chemically crosslinked nanoparticle network gels are created either by functionalizing the microgel precursor polymers with secondary complementary crosslinkable groups or via the addition of a small molecule crosslinker. For example, adipic dihydrazide has been used to covalently crosslink a network of pNIPAM-co-acrylic acid microgels while or glutaric dialdehyde has been used to crosslink a network of pNIPAM-co-allylamine microgels.[86]

Alternately, nanoparticles can be used as crosslinkers for other types of hydrogel networks. Most reported examples of nanoparticle-crosslinked morphologies are constructed based on inorganic nanoparticle crosslinkers such as mineral clays,[89] gold nanoparticles[90] or quantum dots.[91] However, there are some examples of nanogels being used as the crosslinking nanoparticle. In one such example, oxidized cholesterol-modified starch nanoparticles (OCS) with aldehyde groups were used as a crosslinker for poly(vinyl amine) to create a hydrogel network via Schiff-base formation. These gels showed increasing swelling with increasing pH, a property leveraged to almost completely release the drug doxorubicin at pH =3-5 but nearly no release at pH=7 within 125 hours; this release profile is beneficial for cancer tumor therapy, since tumour tissue environments are typically acidic.[92]

The use of linear starch as a crosslinker has been extensively reported in conjunction with multiple reports for modifying starches with various crosslinkable groups. These crosslinking motifs typically comprise of complementary groups which can “click” together, or incorporating charged groups to allow for pH- responsive ionic crosslinking. By adding vinyl group units, a molecule can actively engage in free radical chemistry to graft monomer units to the functionalized starch.[73-75, 93-95] This approach is particularly used to create at least partially degradable hydrogels, leveraging the

enzymatic degradability of the starch crosslinking component. One such example of a successfully applied modified starch is described by Hedin et al., who used the C6 hydroxyl group on starch to epoxide ring open glycidyl methacrylate in DMSO. This successfully imparts a methacrylic group on the starch backbone (DS = 0.08 in this case), enabling UV curing to create a hydrogel. They report the formation of hydrogels based on 1, 5, and 10% solutions of the modified starch, with the opacity of the 5 and 10% solutions disappearing during gelation to result in a clear hydrogel.[96]

A prime example of starch being used effectively to create a hydrogel is described by San Román et al. They report a xerogel made by reactive extrusion of a blend of starch, acrylic acid and acrylamide monomers crosslinked using bisacrylamide, resulting in successful polymer grafting on the starch. These gels have been shown to degrade to 40% of its original weight within 25 days of immersion in physiological conditions and pH sensitivity.[97] Such a hopeful biomaterial provides precedent for studying starch as a crosslinker, as is can allow for natural degradation through hydrolytic or enzymatic means.

In chapter 2, starch nanoparticles can be encapsulated within a polymer matrix and selectively degraded to leave behind nanopores in the continuous phase. However, the bulk POEGMA-based hydrogel showed clear long-term stability in storage conditions. It would be advantageous to thus leverage this proven capacity for SNP degradation on a crosslinkable SNP that could be eroded enzymatically and thus cause the hydrogel network to break down.[78, 79, 98] Relative to using linear starch as a crosslinker, the use of SNPs as crosslinkers offers potential benefits in terms of localizing the crosslinks in well-defined nanodomains rather than dispersed throughout the network as with linear starch. We hypothesize that such a distribution of crosslinks (i.e. dense crosslinking around the SNPs but relatively loose crosslinking between the SNPs) may be advantageous for promoting gel degradation while still exploiting the inherent elasticity of the SNP to produce hydrogels of useful mechanical strengths.

In this chapter, the potential of a modified thermoplastic starch nanoparticles as crosslinkers to form a hydrogel network will be investigated. Methacrylated SNPs previously investigated in our group will be used as substitutes for EGDMA from the formulation reported in Chapter 2, as shown schematically in **Scheme 3-1**.

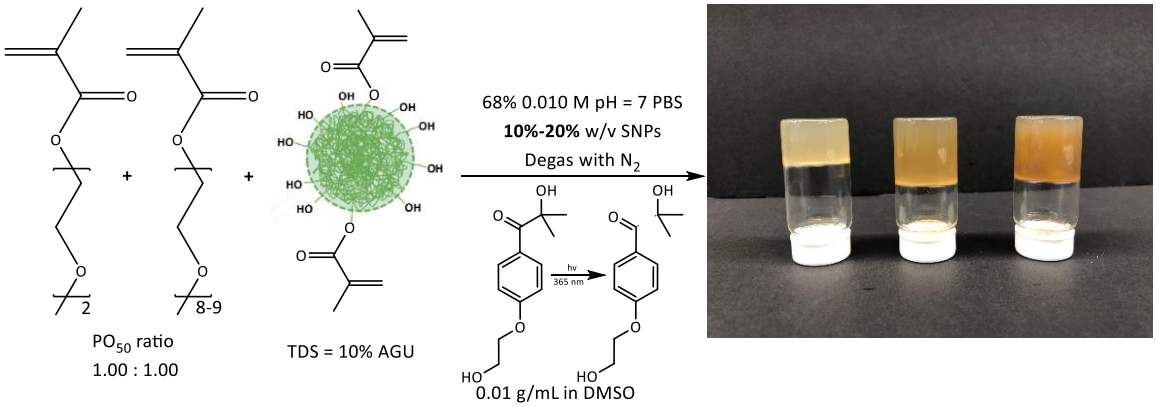

Scheme 3-1. *Reaction scheme for fabrication of UV-PO_{50} hydrogels using varying amounts of methacrylated SNPs, directly replacing EGDMA in the previously described system.*

This chapter will then investigate the key properties of the hydrogels produced (swelling, mechanics) as well as explore the enzymatic degradation of these hydrogels and the effect of SNP degradation on the gel properties. If the modified starch nanoparticle is the only mechanism by which the network is formed and being held together, then exposure to an enzyme would be expected to lead to the total dissolution of the hydrogel into oligomers. This could of relevance for designing a range of biomaterials with well-defined degradation properties.

3.1.1 - Chapter Objectives

- To synthesize an ultraviolet curable hydrogel in which modified SNPs are the exclusive crosslinker, replacing the synthetic crosslinker EGDMA investigated in Chapter 2
- To determine the comparative curing kinetics, mechanical performance and swelling abilities of SNP-crosslinked hydrogels in comparison to EGDMA-crosslinked hydrogels.
- To investigate the impact of enzymatically degrading the functionalized SNP crosslinker on the hydrogel properties.

3.2 - Materials

Experimental grade starch nanoparticles (SNPs) were made and donated by EcoSynthetix, Inc. [Burlington, Ontario].

Poly (ethylene glycol) methyl ether methacrylate with an average molecular weight of 500 g/mol ($OEGMA_{500}$) and di(ethylene glycol) methyl ether methacrylate ($M(EO)_2MA$) [MilliporeSigma, Oakville, Ontario] were filtered through basic alumina to remove the 4-methoxyphenol inhibitor.

Phosphate buffered saline tablets (PBS, 0.01 M phosphate buffer, 0.0027 M potassium chloride and 0.137 M sodium chloride, pH 7.4, at 25 °C) [MilliporeSigma, Oakville, Ontario] were dissolved in 200 mL/tablet of ultrapure Milli-Q grade deionized water (Milli-Q H_2O) to achieve the desired concentrations. The pH of the buffer was checked using a calibrated pH probe.

Deuterium oxide (D_2O) [10 x 1mL ampoules, 99.96% D from Cambridge Isotope Labs, Massachusetts], hydrochloric acid (HCl) [0.1 M, 1.0 M solutions from LabChem, Pennsylvania], sodium hydroxide (NaOH) [0.1 M, 1.0 M solutions from LabChem, Pennsylvania], methacrylic anhydride [MilliporeSigma, Oakville, Ontario], and 2-hydroxy-4′-(2-hydroxyethoxy)-2-methylpropiophenone (Irgacure 2959) [MilliporeSigma, Oakville, Ontario] were used as received.

3.3 - Experimental Methods

3.3.1 - Synthesis of Methacrylate Functionalized Starch Nanoparticle

An aqueous dispersion of 30.0 g of experimental grade SNPs was prepared at 10 %w/v in milli-Q H_2O by vigorous stirring and heating to 60°C. 2.523 mL of methacrylic anhydride was then added in 10 aliquots over 1 hour, maintaining the pH at 10.4 throughout the process. After addition of methacrylic anhydride was completed, the solution was stirred for 30 minutes at pH=11.0, neutralized to pH=7.0, filtered, and dialyzed extensively using a 3.5 kDa MWCO dialysis membrane against milli-Q H_2O for 3 days. The purified product was lyophilized and stored at room temperature in the dark. To assess the degree of methacrylation of the products, 40.0 mg of product was

dissolved in 1 mL deuterium oxide (D_2O) and characterized using ^1H NMR with water signal suppression (Bruker AV 600 MHz spectrometer). These products were denoted as "SNP-MA-0.10", where 0.10 corresponds to the theoretical degree of substitution of methacrylate groups on the SNPs.

3.3.2 - Synthesis of Ultraviolet-Cured Poly (Oligoethylene Glycol Methyl Ether Methacrylate) Hydrogels Crosslinked via Methacrylate Functionalized Starch Nanoparticles

Methacrylate functionalized SNPs prepared in 3.3.1 (SNP-MA-0.10) were suspended at three concentrations (5, 10, or 20%w/v) in 0.01 M PBS. Subsequently, 1 g (2 mmol) of $OEGMA_{500}$, an equimolar amount of ($M(EO)_2MA$) (0.376 g, 2 mmol), and 0.669 mL of a 10 mg/mL dimethyl sulfoxide (DMSO) solution of Irgacure 2959 were added and gelation was conducted as described in section 2.3.2.2.

3.3.3 - Ultraviolet Curing Rheology

Rheology experiments of precursor solution properties as well as UV-*induced in situ* gelation were conducted using a TA Instruments Discovery Hybrid Rheometer Mark 2 equipped with a UV accessory, as described in section 2.3.3.

3.3.4 - Swelling Kinetics

Precursor solutions cast in pre-punched 5/8" hole in a ¼'' thick silicone sheet and then photopolymerized for 20 minutes using a Con-Trol-Cure Cure Zone 2 UV Flood Curing System equipped with a 400 W metal halide light source which outputs 80 mW/cm^2 of 365 nm long-wave ultraviolet light. Gels were equilibrated overnight in 100% humidity and then loaded into cell culture inserts with the tab cut off and placed in a 6-well plate filled with 12 mL of 0.01 M PBS. Gravimetric swelling measurements were collected every 15 minutes for the first hour, every 30 minutes for the next 2 hours, every hour for the next 6 hours, and then daily until the end of the measurement

period. Wells were filled with 12 mL 0.01 M PBS, ensuring that each gel is fully submerged in the PBS solution. All swelling measurements were done in triplicate.

3.3.5 - Degradation Study

3.3.5.1 - SNP-MA Degradation Strategy

Two methods of enzymatic degradation of the SNP-based crosslinkers were assessed. In the first method, 10 mg of α-amylase was added to the aqueous phase of the prepolymer solution and entrapped inside the gel during photopolymerization; following, the gels were swollen in 0.01 M PBS at 70°C for 16 hours to activate the enzyme. In the second method, gels were prepared as described in section 3.3.2 and then swollen in a 1%w/v solution of α-amylase in 0.01 M PBS at 70°C for 16 hours to activate the enzyme.

3.3.5.2 - Mechanical Testing

Mechanical testing as a function of amylase degradation time was performed on the SNP-MA-0.1 hydrogels using a CellScale MicroSquisher. The cantilever was made by affixing a 4 mm x 4 mm platen to a 406 µm diameter cantilever. A hydrogel with dimensions of ½" diameter x 1/8" height was loaded on a glass cover slip before being placed in the test chamber, which was then filled with 1%w/v solution of α-amylase in 0.01 M PBS pre-warmed to 70°C. A compressive force measurement was conducted before swelling (i.e. on the as-prepared gel), at the beginning of swelling (i.e. immediately after the amylase PBS solution was added), every hour for the next 2 hours, and once the following day to track the mechanics of the gel as a function of the amylase incubation time. The resulting force as a function of time using an indentation speed of 0.005 mm/s for 100 seconds (corresponding to ~40% compression).

3.4 - Results & Discussion

3.4.1 - Quantitative Characterization of Methacrylated Starch Nanoparticles

Proton nuclear magnetic resonance spectroscopy (^{1}H NMR) was used to determine the degree of methacrylation on SNPs, the result of which is shown **in Figure 3-1**. This experiment was run using a water signal suppression technique to reduce the magnitude of the signal associated with water present in the sample that is tightly bound to the starch, allowing for SNP backbone signals to be observed.

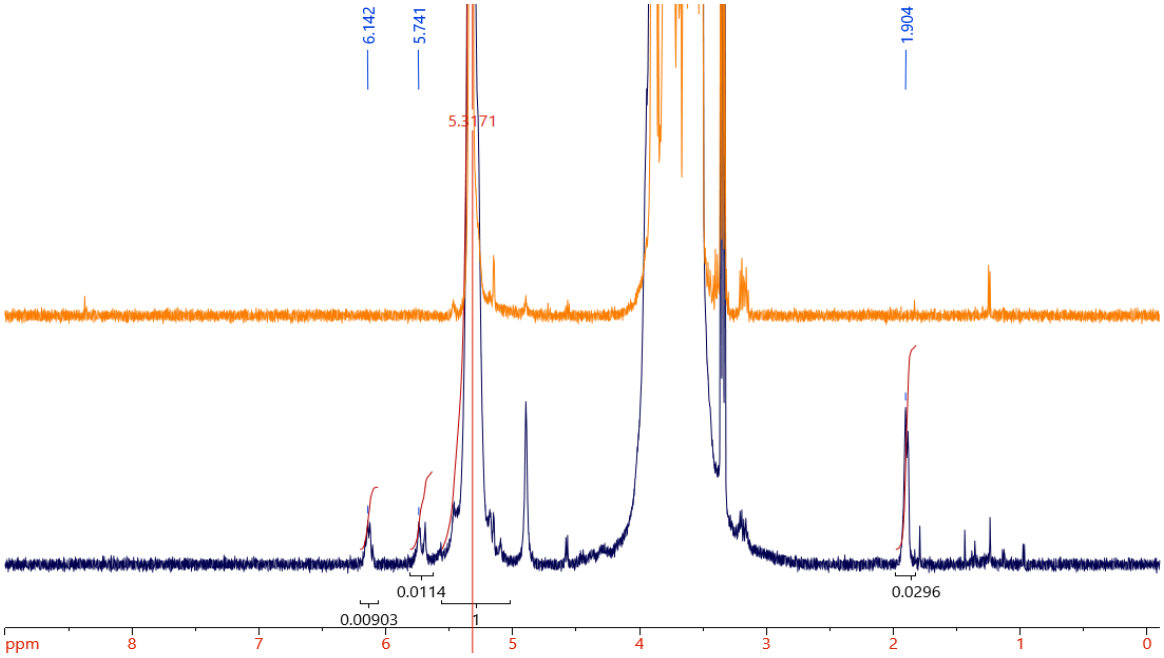

Figure 3-1. *^{1}H NMR of experimental grade SNPs (●) and SNP-MA-0.10 (●).*

Three new characteristic peaks appeared in the SNP-MA-0.1 spectrum: a singlet at ~1.9 ppm, (corresponding to the methyl group from the methacrylate moiety) and two equivalent magnitude peaks at ~5.7 and ~6.1 ppm (corresponding to the diastereotopic protons on the C=C bond that are constrained in free rotation by the double bond, resulting in them being exposed to similar but different electronic environments). Comparing the integral values of the diastereotopic protons to that of the methyl singlet, each diastereotopic proton individually shows in 1/3 of the signal of the

methyl group, accounting for all 5 new protons in the expected stoichiometry. By comparing these intensities to that of the anomeric proton peak at ~5.3 ppm (characteristic of one distinct proton per repeat unit in the polymeric starch backbone), an experimental DS = 0.009 was observed. This DS value is substantially lower than the theoretical DS = 0.10 based on the methacrylation recipe used and can be explained due to the tendency of methacrylic anhydride to hydrolyze into two equivalents of methacrylic acid in the basic conditions used for the methacrylation reaction, a side reaction that consumes part of the anhydride reagent. This side-reaction may be suppressed by performing the reaction in an aprotic solvent compatible with SNPs such as DMSO; however, this would require a more rigorous purification step, and previous starch hydrogel papers have indicated that DS values of 0.08 or lower can facilitate effective photopolymerization into hydrogels.[96]

3.4.2 - Photorheology Results

Photorheology was used to assess the effect of varying the concentration of methacrylated SNP crosslinkers within the UV-POEGMA system on the curing time and mechanical performance of the resulting hydrogel, with the results shown in **Figure 3-2**.

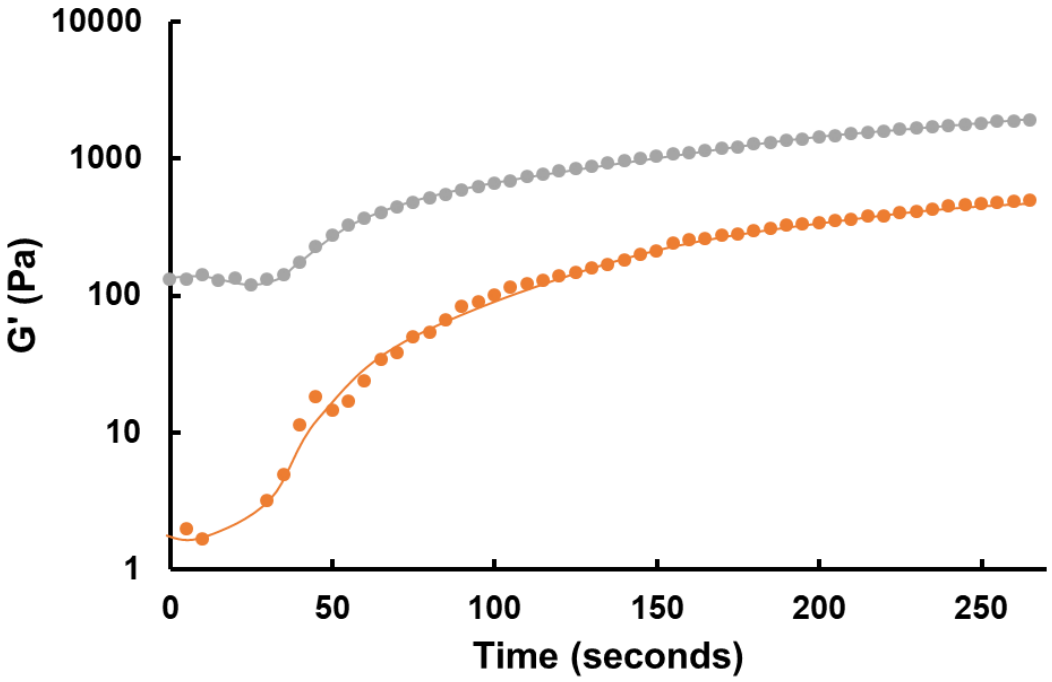

Figure 3-2. *Photorheology results for hydrogels prepared using SNP-MA-0.1 as a crosslinker in UV-PO$_{50}$. 10%w/v (●), 20%w/v (●). Lines are to guide the eye.*

Note that a fourth concentration of 30%w/v SNP-MA was also attempted but resulted in significant phase separation with the POEGMA gel components; as such, 20%w/v (corresponding to 0.56 g SNP-MA/g POEGMA) was determined to be the maximum incorporation limit.

5%w/v SNP-MA-0.1 was unable to form a detectable gel, maintaining a semi-viscous product over the full photogelation process with a G' value within the instrument noise. However, increasing the concentration to at least 10%w/v, a gel began forming immediately after exposure to UV (at the 30 s time point in **Figure 3-2**) and reached a plateau modulus of ~1150 Pa within 240 seconds. Increasing the concentration further to 20%w/v SNP-MA-0.1 resulted in an increase of the plateau storage modulus to ~3700 Pa while maintaining similar curing kinetics.

The onset and gelation times are similar to those observed with the EGDMA-crosslinked hydrogels with network formation occurring within <40 s following UV irradiation and reaching maximum strength within 4-5 minutes. However, while the initial pre-curing strength of the EGDMA crosslinked polymer gels ranged narrowly between 10-50 Pa, the 10%w/v SNP-MA-0.1 precursor solution has a G' value of ~100 Pa while the 20%w/v SNP-MA-0.1 precursor solution has an initial G' of ~1000 Pa. This result is attributable to the potential to use higher concentrations of methacrylated SNPs in the formulations given that their capacity to crosslink avoids the phase separation observed in the SNP-entrapped gels upon photopolymerization**.** However, the maximum achievable G' of the SNP-MA-0.1 crosslinked hydrogels is lower than can be achieved with EGDMA given the steric limitations inherent in using a macromolecular, particulate-based crosslinker relative to a highly soluble, small molecule divalent crosslinker.

3.4.3 - Swelling Kinetics

The swelling responses of SNP-MA-UV-POEGMA hydrogels in 0.01 M PBS as a function of time are shown in **Figure 3-3.**

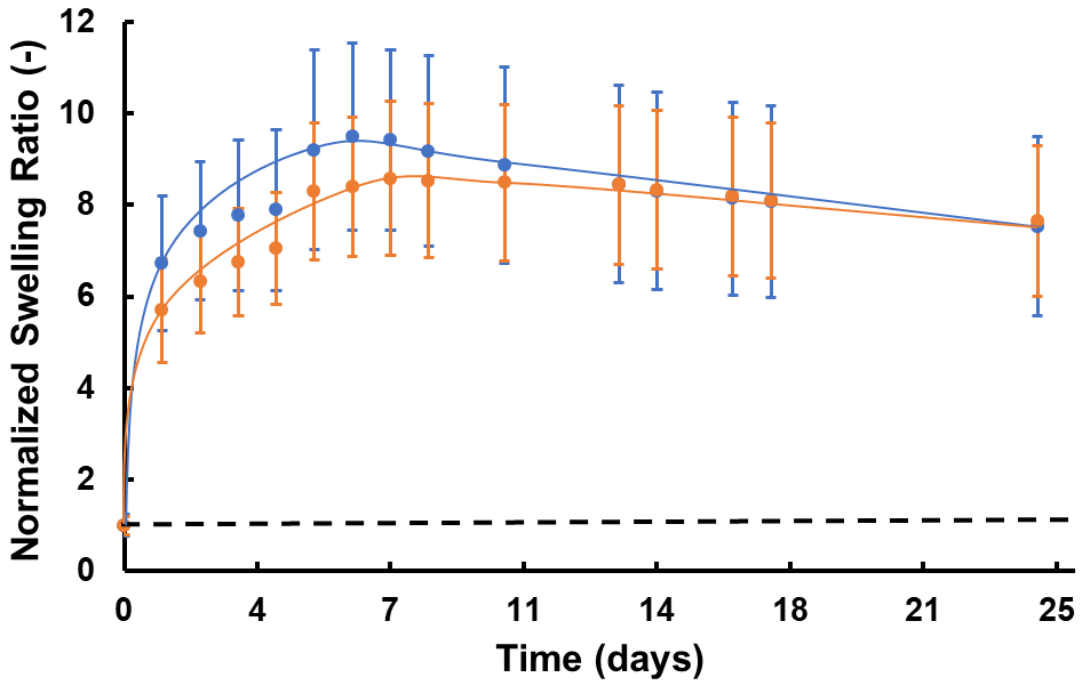

Figure 3-3 *Normalized swelling results for UV-PO$_{50}$ gels made with varying concentrations of 0.1-SNP-MA as crosslinker: 10%w/v (●), 20%w/v (●). Lines are to guide the eye.*

There was no significant difference observed in swelling kinetics or equilibrium degree of swelling as a function of the amount of SNP-MA crosslinker used. We hypothesize this observation is explained by the counterbalancing of the solvent mixing effects (i.e. higher swelling capacity when more SNPs are added) and the crosslinking effects (i.e. lower swelling capacity as more methacrylated SNPs can crosslink the network). Both gels can swell between 8-10 times their initial weights, significantly higher than that achieved with EGDMA-crosslinked hydrogels with similar mechanics (e.g. UV-PO_{50}-1.0wt% unD-SNP showed a G' value of 2900 Pa (**Figure 2-2**) but a swelling ratio of 1.65 (**Figure 2-5**)). Indeed, the small spike in water content observed after four days was a result of the gels imbibing all the water in well, such that further swelling was observed upon refilling the well with PBS. As such, the SNP-MA-crosslinked hydrogels exhibit extremely high swelling ratios while still maintaining at least moderate overall mechanics.

3.4.4 - Degradation Study

3.4.4.1 - Qualitative Consequences of SNP Crosslinker Degradation

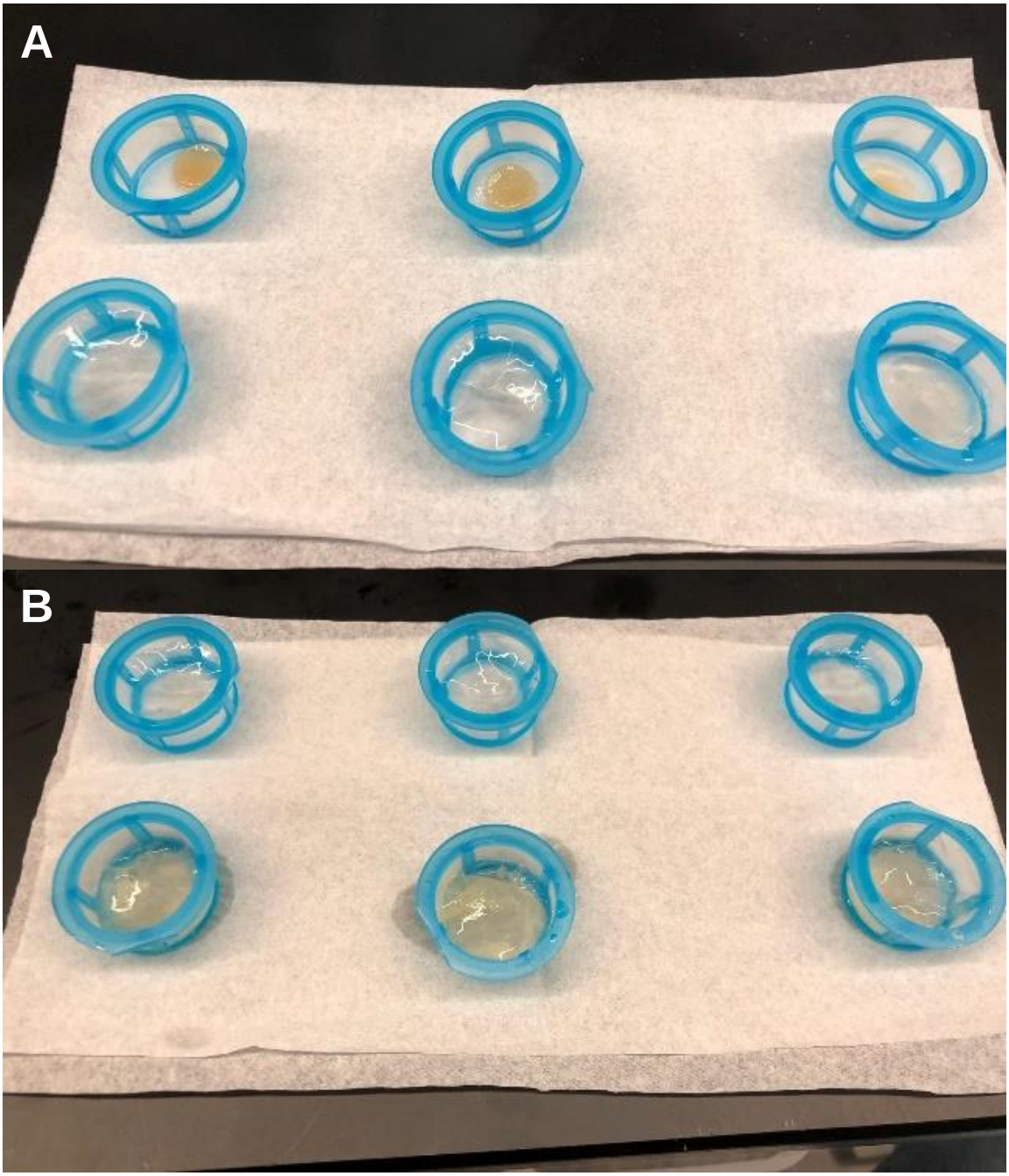

Figure 3-4. *Qualitative swelling of SNP-MA-0.1 crosslinked hydrogels under different conditions.* ***Top row:*** *unswollen UV-PO_{50}-20 w/v%-SNP-MA-0.1 gels****; 2nd row:*** *UV-PO_{50}-20 w/v%-SNP-MA-0.1 gels swollen in 0.01 M PBS;* ***3rd row:*** *UV-PO_{50}-20 w/v%-SNP-MA-0.1 gels with 0.1%w/w of α-amylase swollen in 0.01 M PBS.* ***Bottom row:*** *UV-PO_{50}-20 w/v%-SNP-MA-0.1 gels swollen in 1 w/v% α-amylase in 0.01 M PBS.*

The effect of enzymatically degrading the SNP-MA-0.1 crosslinker is shown qualitatively in **Figure 3-4**. We hypothesized that if the SNP-MA was degraded, the entire gel would fall apart, as the functionalized particles are the only mechanism by which the POEGMA polymer chains can be networked. **Figure 3-4** shows qualitative comparisons between SNP-MA-0.1 crosslinked hydrogels as prepared (top row), swollen in 0.01 M PBS (2nd row), encapsulated with amylase (3rd row), or treated post-gelation with amylase (bottom row). After 16 hours of swelling in 1%w/v amylase solution, a significantly smaller amount of weaker gel was left over compared to the same gel swollen for 16 hours in enzyme-free 0.01 M PBS. This result suggests that the SNP crosslinker can be selectively degraded via amylase exposure. However, full dissolution of the gel was not observed over the tested degradation period. Note that the amylase encapsulation experiment conducted at room temperature resulted in no noticeable gel curing after 20 minutes of curing, with the samples still liquid-like and similar to the pre-gel solution. As such, to produce the gels shown in the 3rd row of Fig. 3-4, the prepolymer solution was kept cold to mitigate any premature degradation of the SNPs via residual amylase activity at room temperature.

3.4.4.2 - Mechanical Testing

The impact of enzymatic degradation of the SNP-based crosslinkers was quantitatively assessed by mechanical testing. Initially, a stress relaxation test of a pre-compressed gel was attempted using the Mach-1 micromechanical tester. However, this testing proved to be difficult to conduct on these gels as they were very soft (particularly after degradation) and the indenter would go through the gel without detecting a normal force. Instead, the highly sensitive cantilever-based compression testing achievable using the MicroSquisher was employed to track the time course of gel mechanics, with the added advantage of enabling the gel to be incubated in solvent throughout the experiment. Optical images of the test gel, shown in **Figure 3-5A-E**, show the gel swelling slowly as the media penetrates into the gel, with degradation making the gel more transparent over time.

As such, compressive modulus measurements were consistently conducted in the center of each gel to ensure the results are not biased by the penetration speed of the enzyme into the gel.

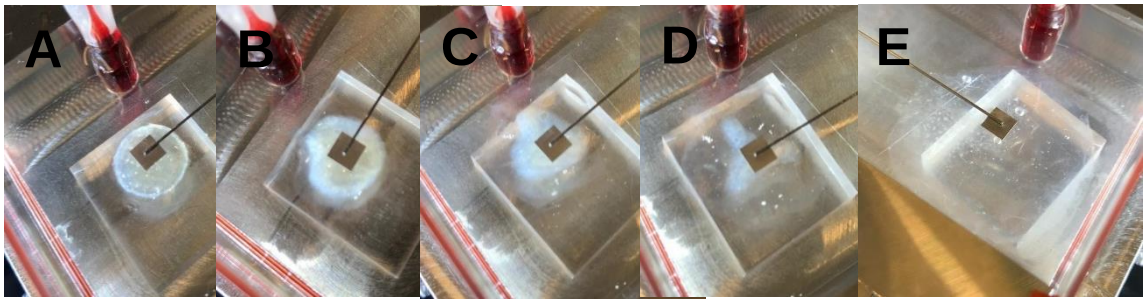

Figure 3-5. *Optical images of UV-PO_{50}-20 w/v%-SNP-MA-0.1 loaded on the MicroSquisher mechanical tester while swelling in 1.0%w/v α-amylase in 0.01 M PBS solution at time (t)* **A.** *0 hours.* **B.** *1 hour.* **C.** *2 hours.* **D.** *3 hours.* **E.** *18 hours.*

The corresponding force versus distance displacement data is shown in **Figure 3-6A-B**. Before swelling, the gel shows a linear force versus distance response, reaching a normal force of up to 55 mN at 40% compression. Immediately after adding the swelling media, the modulus of the gel noticeably decreases, with further decreases (particularly at the outer periphery of the gel) observed at longer times as the gel continues to imbibe the surrounding media; indeed, the normal force decreases to nearly 0 mN after swelling overnight. However, similar degradation profiles were observed between amylase-treated samples and samples swollen with 0.01 M PBS (no amylase). While this result on the surface indicates that amylase cannot efficiently degrade the SNP

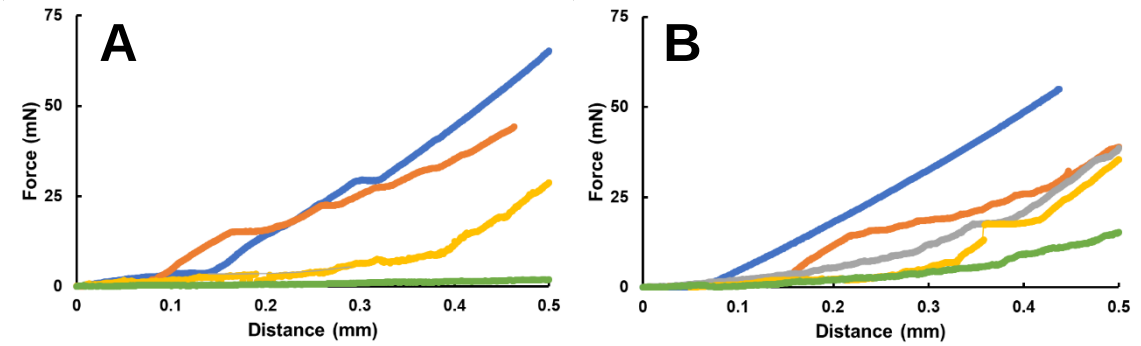

Figure 3-6. *MicroSquisher force versus distance curves for the compression of UV-PO_{50}-20 w/v%-SNP-MA-0.1 hydrogels at different time points* ***A.*** *swollen in 0.01 M PBS. Before swelling (●), t_0 (●), t = 1 hour (●), 16 hours (●)* ***B.*** *following incubation with 1.0%w/v α-amylase in 0.01 M PBS. Before swelling (●), t_0 (●), t = 1 hour (●), t = 2 hours (●), t = 16 hours (●).*

crosslinkers, there were several experimental uncertainties that make this conclusion unclear. First, since the CellScale MicroSquisher was not equipped with a heating element and the optimal temperature for amylase degradation to occur is between 65-70°C, the amylase was optimally

active at the beginning of the swelling but would rapidly reduce in activity to ~20% of the high temperature condition upon cooling to room temperature.[99] Second, the gels would often slip from under the cantilever, manifesting as slips or no detection of normal force at all in the data; increased confinement of the gel may moderate this challenge. Third, it is possible that the very large inherent swelling ratio observed with these hydrogels makes the gels too weak such that the mechanical testing approach is too insensitive to discriminate between SNP degraded and non-degraded hydrogels.

3.5 – Conclusions

3.5.1 – Conclusions

Methacrylated SNPs were shown to be useful as the exclusive crosslinker for a POEGMA hydrogel. These gels have a storage modulus of 1-5 kPa after UV curing and are able to swell up to 10x their weight in 0.01 M PBS. The ability of these gels to swell to a great extent was attributed to changing the crosslinking distribution by using the SNPs instead of a small molecule such as EGDMA, since the particles create localized domains of crosslinking. While some evidence for the degradation of the SNP crosslinker was observed, quantification was challenging.

This sort of gel can have benefits in tissue engineering applications given their tunable degradation and mechanical strength over time. These gels may also have context in environmental applications where their high swellability and subsequent degradation could be leveraged.

3.5.2 – Summary

- SNPs can be functionalized with methacrylate groups and used as crosslinkers in a POEGMA-based hydrogel network at concentrations between 10-20%w/v, corresponding to 0.28-0.56 g SNP/g POEGMA.
- Methacrylated SNP crosslinked hydrogels begin curing within 10 s following irradiation, fully cure within ~ 4 minutes, and can achieve storage moduli of >1 kPa.
- The resultant gels can swell up to 10x by weight in 0.01 M PBS

- Degradation can be induced with the introduction of α-amylase but complete degradation (i.e. complete gel dissolution) was not observed on the time scale of the experiment. Further studies must be done to confirm effect of enzymatic degradation.

3.6 - References

1. Poorgholy, N.; Massoumi, B.; Jaymand, M., A novel starch-based stimuli-responsive nanosystem for theranostic applications. *Int. J. Biol. Macromol.* **2017,** *97*, 654-661.
2. Hamidi, M.; Azadi, A.; Rafiei, P., Hydrogel nanoparticles in drug delivery. *Adv Drug Deliv Rev* **2008,** *60* (15), 1638-49.
3. Hirakura, T.; Nomura, Y.; Aoyama, Y.; Akiyoshi, K., Photoresponsive nanogels formed by the self-assembly of spiropyrane-bearing pullulan that act as artificial molecular chaperones. *Biomacromolecules* **2004,** *5* (5), 1804-1809.
4. Hu, Z. B.; Xia, X. H., Hydrogel nanoparticle dispersions with inverse thermoreversible gelation. *Adv. Mater.* **2004,** *16* (4), 305-+.
5. Huang, G.; Gao, J.; Hu, Z.; St John, J. V.; Ponder, B. C.; Moro, D., Controlled drug release from hydrogel nanoparticle networks. *J. Control. Release* **2004,** *94* (2-3), 303-11.
6. Fang, Y. Y.; Wang, L. J.; Li, D.; Li, B. Z.; Bhandari, B.; Chen, X. D.; Mao, Z. H., Preparation of crosslinked starch microspheres and their drug loading and releasing properties. *Carbohydr. Polym.* **2008,** *74* (3), 379-384.
7. Hu, Z. B.; Xia, X. H.; Marquez, M.; Weng, H.; Tang, L. P., Controlled release from and tissue response to physically bonded hydrogel nanoparticle assembly. *Macromolecular Symposia* **2005,** *227* (1), 275-284.
8. Guler, M. A.; Gok, M. K.; Figen, A. K.; Ozgumus, S., Swelling, mechanical and mucoadhesion properties of Mt/starch-g-PMAA nanocomposite hydrogels. *Applied Clay Science* **2015,** *112*, 44-52.
9. Skardal, A.; Zhang, J.; McCoard, L.; Oottamasathien, S.; Prestwich, G. D., Dynamically crosslinked gold nanoparticle - hyaluronan hydrogels. *Adv. Mater.* **2010,** *22* (42), 4736-40.
10. Molina, M.; Asadian-Birjand, M.; Balach, J.; Bergueiro, J.; Miceli, E.; Calderón, M., Stimuli-responsive nanogel composites and their application in nanomedicine. *Chem. Soc. Rev.* **2015,** *44* (17), 6161-6186.
11. Li, Y.; Liu, C.; Tan, Y.; Xu, K.; Lu, C.; Wang, P., In situ hydrogel constructed by starch-based nanoparticles via a Schiff base reaction. *Carbohydr. Polym.* **2014,** *110*, 87-94.
12. Avval, M. E.; Moghaddam, P. N.; Fareghi, A. R., Modification of starch by graft copolymerization: A drug delivery system tested for cephalexin antibiotic. *Starch-Starke* **2013,** *65* (7-8), 572-583.
13. Chen, Q.; Yu, H. J.; Wang, L.; ul Abdin, Z.; Chen, Y. S.; Wang, J. H.; Zhou, W. D.; Yang, X. P.; Khan, R. U.; Zhang, H. T.; Chen, X., Recent progress in chemical modification of starch and its applications. *Rsc Advances* **2015,** *5* (83), 67459-67474.
14. Chiu, C.; Solarek, D., Modification of Starches. In *Starch: Chemistry and Technology*, Third Edition ed.; Elsevier inc.: 2009; p 27.
15. Kaur, B.; Ariffin, F.; Bhat, R.; Karim, A. A., Progress in starch modification in the last decade. *Food Hydrocolloids* **2012,** *26* (2), 398-404.
16. Moad, G., Chemical modification of starch by reactive extrusion. *Prog. Polym. Sci.* **2011,** *36* (2), 218-237.
17. Tomasik, P.; Schilling, C. H., Chemical Modification of Starch. In *Advances in Carbohydrate Chemistry and Biochemistry Volume 59*, 2004; pp 175-403.
18. Hedin, J.; Ostlund, A.; Nyden, M., UV induced cross-linking of starch modified with glycidyl methacrylate. *Carbohydr. Polym.* **2010,** *79* (3), 606-613.
19. Elvira, C.; Mano, J. F.; San Roman, J.; Reis, R. L., Starch-based biodegradable hydrogels with potential biomedical applications as drug delivery systems. *Biomaterials* **2002,** *23* (9), 1955-1966.
20. Araujo, M. A.; Cunha, A. M.; Mota, M., Changes in morphology of starch-based prothestic thermoplastic material during enzymatic degradation. *J. Biomater. Sci. Polym. Ed.* **2004,** *15* (10), 1263-80.

21. Azevedo, H. S.; Reis, R. L., Encapsulation of alpha-amylase into starch-based biomaterials: an enzymatic approach to tailor their degradation rate. *Acta Biomater.* **2009,** *5* (8), 3021-30.
22. Butterworth, P. J.; Warren, F. J.; Ellis, P. R., Human α-amylase and starch digestion: An interesting marriage. *Starch - Stärke* **2011,** *63* (7), 395-405.
23. Konsula, Z.; Liakopoulou-Kyriakides, M., Hydrolysis of starches by the action of an α-amylase from Bacillus subtilis. *Process Biochem.* **2004,** *39* (11), 1745-1749.

4 Conclusions & Future Directions

4.1 – Physically Entrapped SNPs in UV-Cured POEGMA Hydrogels

4.1.1 – Summary & Objective Review

- ✓ To synthesize an ultraviolet-curable hydrogel matrix which can entrap SNPs
- ✓ To perform performance testing and material optimization by studying key parameters affecting gel properties
- ✓ To selectively degrade SNPs to create macroporous structures and characterize the properties of the new macroporous hydrogel materials.

In reviewing the goals set out in the chapter, many of the main objectives were achieved. A bulk hydrogel cured using UV light was fabricated and studied for its ability to incorporate prefabricated SNPs as a nanocomposite. Characterization of the mechanics and swelling of various systems indicated that hydrogels prepared with a 50/50 ratio of long/short-chain monomers with a 2:1 monomer:crosslinker ratio gave the optimal hydrogel properties. The effect of SNP concentration was also investigated, with the maximum incorporation of SNP determined to be 1-5%w/v; higher concentrations result in phase separation and decreased storage modulus.

Subsequently, dialyzed SNPs were shown to be selectively degradable from the POEGMA phase using α-amylase, as the degradation products of oligomeric starch fragments and glucose monomers were observed in the supernatant of a swelling solution. Results indicate removal of up to >70% of the original amount of starch inside the hydrogels, with both encapsulated amylase (yielding primarily oligomeric starch products) and soaking in amylase solutions (yielding primarily monomeric glucose) showing the best starch removal potential. Swelling the hydrogel in a 1%w/v amylase solution to induce erosion of the SNPs enabled an effective doubling of the gel's capacity to uptake methylene blue, a result attributable to the increased surface area (adsorption) and free volume (absorption) produced upon the erosion of the SNPs.

4.1.2 – Future Directions

Although many parameters of the UV-cured POEGMA hydrogels described in Chapter 2 were studied, many still could have the potential to show tunablility of properties such as swelling or mechanical performance. A study can be conducted to use a crosslinker with longer chain lengths such as poly (oligo ethylene glycol) di methacrylates with increasing MW from 550 to 20000 g/mol (compared to the 200 g/mol EGDMA used in this study), which is expected to result in a looser network structure that may make removal of starch via enzymatic degradation easier.

Another potential optimization lies around the initiator species used in the formulation. Alternatively, lithium phenyl-2,4,6-trimethylbenzoylphosphinate (LAP) has been used favorably over Irgacure 2959 as the initiator for photopolymerization due to its enhanced water solubility and proven non-cytotoxicity. This initiator has also been proven as effective as Irgacure 2959 at lower concentrations since it has a much better absorbance for 365 nm light as well as other wavelengths >400 nm, enabling curing under milder conditions that can help promote cell viability.[1] Many of the resultant hydrogels using this initiator have been shown to be effective as tissue scaffolds. [2] Adding porosity to similar PEG gels made with this initiator showed increased cell viability,[3] making the *in situ* degradability of SNPs potentially attractive for enhancing the material performance in that application.

It would also be interesting to further investigate the gel morphologies created in this study. Although the nanoporosity of the gels was probed using the methylene blue assay, further inquiry should be done to see the subtle differences between blank gels, swollen gels, entrapped SNPs in the gels, and their subsequent degradation. Electron microscopy may be an effective method to inspect these gels but is likely to include observation of pseudo-pores created as artifacts from freezing the sample (as is required for lyophilization and drying of the sample for SEM analysis), pores that cannot be explicitly differentiated from the created nanoporous structure. A more effective method for probing the internal structure of a hydrogel is small angle neutron scattering (SANS). This has previously been done annually in the group at the National Institute of Standards

and Technology (NIST) Center for Neutron Research. McMaster is currently commissioning an instrument capable of doing these experiments. In such experiments, the hydrogel would be irradiated with a neutron beam and the resulting scattering profile of the neutrons can be analyzed using appropriate models to probe internal nanomorphologies with length scales on the range of 1-10000 nm. These measurements can help establish the understandings of the domain formation and biphasic interactions between the POEGMA and SNPs.

Since it has been shown that POEGMA polymers prepared with an appreciable fraction of short chain comonomer can deswell when heated above their LCST, the temperature response of the SNP-impregnated thermoresponsive POEGMA hydrogels should be investigated. Such responsiveness may be relevant to creating a drug delivery vehicle, as the secondary deswelling mechanism (temperature) after a primary degradation mechanism (amylase degradation of SNPs) may offer potential for creating dual environmentally-responsive release systems featuring slow release observed from internal degradation of the SNPs followed by a final burst release when the gel is heated.

The potential of these gels should also be tested for their injectability, since UV biomedical applications are generally limited due to harsh UV intensity and ineffective penetration above surface levels of tissue. This would generally limit the application of such materials. However, if this material proves to be injectable, it can be applied similarly to the example provided by Bourban et al., who used a device where a fiber optic cable was feed through a connector joint with the prepolymer solution to effectively irradiate the prepolymer solution during injection and within the cavity, allowing for effective photogelation and replacement of the nucleus pulposus tissue in

intervertebral discs, as pictured in **Figure 4-1**. Such a device can be fabricated with expertise on campus.

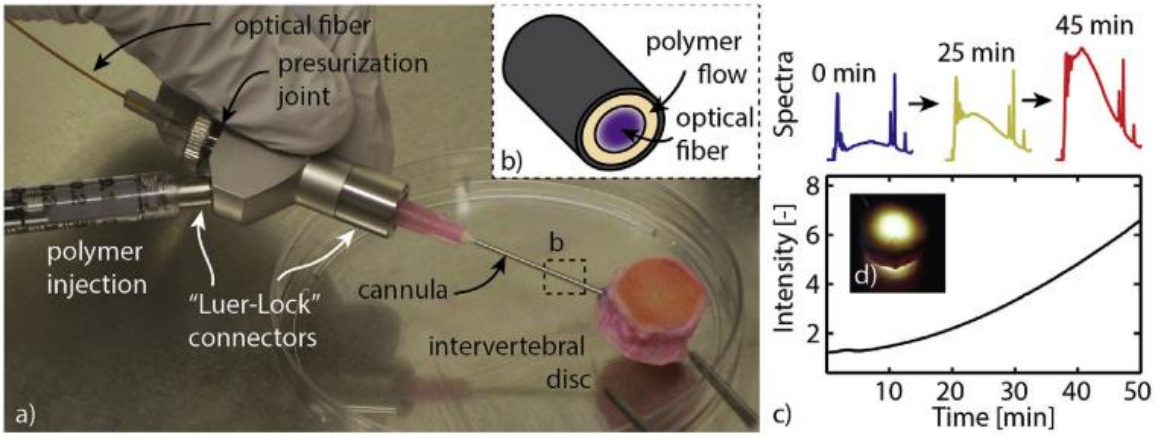

Figure 4-1. *Photogelation set-up for the delivery of UV-cured hydrogels as injectable tissue replacement in intervertebral discs. Adapted with permission from Pioletti et al.*

4.2 – Methacrylate-Functionalized SNP-Mediated Crosslinking of UV-Cured POEGMA Hydrogels

4.2.1 – Summary & Objective Review

- ✓ To synthesize an ultraviolet curable hydrogel in which modified SNPs are the exclusive crosslinker, replacing the synthetic crosslinker EGDMA investigated in Chapter 2
- ✓ To determine the comparative curing kinetics, mechanical performance and swelling abilities of SNP-crosslinked hydrogels in comparison to EGDMA-crosslinked hydrogels.
- o To investigate the impact of enzymatically degrading the functionalized SNP crosslinker on the hydrogel properties.

The goals in this chapter were partially achieved, with questions remaining about the penultimate result of the hydrogel degradation. Functionalized SNPs with methacrylate groups were shown to be an effective substitute for the EGDMA crosslinker used in Chapter 2, with gels forming at SNP concentrations of 10-20%w/v (corresponding to 0.28-0.56 g SNP/g POEGMA). These gels had similar performance to their SNP-entrapped EGDMA analog, showing up to 3700 Pa storage moduli and similar curing kinetics. However, these SNP-grafted gels were able to swell to 8-10 times its initial fabrication weight, compared to the less than two-fold increase for the nanocomposite system.

Thus, the localization of the crosslinks at the nanoscale impregnated phase, coupled with the higher hygroscopicity of the hydrogels given the higher SNP contents achievable via crosslinking compared to physical impregnation (in which SNP phase separation poses an ongoing challenge), resulted in significantly different swelling behaviours without significantly changing the mechanics.

The final goal of this study around investigating the degradation of the networks upon amylase treatment proved to be difficult to investigate given the nature of the gel. The best attempts were reported qualitatively using optical images and a pilot investigation using MicroSquisher mechanical testing. This study was able to show a decrease in compressive performance over time swollen but was not able to effectively discern any effect of amylase degradation relative to the inherent loss in compressive strength due to the very large degree of swelling observed even in PBS alone. This result is most likely be attributed to the inability of the instrument to keep the amylase at its optimal temperature for digestion for long enough to degrade the SNPs.

These hydrogels have proven to be a unique and interesting material to study, as they go from a clearly immiscible prepolymer solution to an arranged semi-homogenous network upon photogelation. Since SNPs can act as effective crosslinkers while still allowing for a drastic increase in swelling ability, these gels can find application in environmental or tissue engineering applications as well as potential sorbency applications in (for example) personal care products.

4.2.2 – Future Directions

The degradation results for the gels described in Chapter 3 wherein functionalized SNPs were used as the exclusive crosslinker were inconclusive. The MicroSquisher results showed no difference in the described gels when swollen in 0.01 M PBS or a subsequent 1%w/v α-amylase solution when comparing compressive normal force over time. This proves the continued need for probing the effect of thermo-degradation of the SNP crosslinker on the overall hydrogel's modulus.

As mentioned in section 4.1.1, these gels may exhibit thermoresponsive behavior such that their swelling should be evaluated as a function of temperature. Using SANS would also similarly help

understand the role of the SNPs as networking phase from an immiscible phase to part of the continuous phase.

In future studies, the supernatant of the degradation event stage should be assessed for its starch and glucose content as described by the appropriate assays in chapter 2. Other degradation studies should also be conducted using enzymes that can target the amylopectin domains linked by α-[1,6]-glycosidic bonds, instead of (or in addition to) the α-[1,4]-glycosidic bonds linking the linear amylose domains targeted by α-amylase. Using only α-amylase might explain the ability of the gel to resist complete dissolution, since the amylopectin domains in the SNPs can in theory stay intact. Using a non-selective enzyme or combination of enzymes might allow for complete dissolution of this gel. Such a cocktail can be tailored to mimic other enzymatic environments found in nature such as in the body or in plants, allowing for effective study of the applicability of these hydrogels as a biomaterial. The response to these gels against hydrolytic degradation should also be assessed.

In the context of biomaterials, these unique hydrogels should be tested for their cytotoxicity and cellular viability. Such studies would be meaningful in terms of applying these hydrogels as tissue scaffolds. It would also be interesting to probe the protein adsorption capacity of the gels, an indicator of how cells would adhere to the network and/or the potential responses of biomaterials to other protein environments such as blood.

4.3 – References

1. Fairbanks, B. D.; Schwartz, M. P.; Bowman, C. N.; Anseth, K. S., Photoinitiated polymerization of PEG-diacrylate with lithium phenyl-2,4,6-trimethylbenzoylphosphinate: polymerization rate and cytocompatibility. *Biomaterials* **2009,** *30* (35), 6702-7.
2. Lin, C. C.; Anseth, K. S., Cell-cell communication mimicry with poly(ethylene glycol) hydrogels for enhancing beta-cell function. *Proc. Natl. Acad. Sci. U. S. A.* **2011,** *108* (16), 6380-5.
3. Lin, H.; Zhang, D.; Alexander, P. G.; Yang, G.; Tan, J.; Cheng, A. W.; Tuan, R. S., Application of visible light-based projection stereolithography for live cell-scaffold fabrication with designed architecture. *Biomaterials* **2013,** *34* (2), 331-9.

4. Schmocker, A.; Khoushabi, A.; Frauchiger, D. A.; Gantenbein, B.; Schizas, C.; Moser, C.; Bourban, P. E.; Pioletti, D. P., A photopolymerized composite hydrogel and surgical implanting tool for a nucleus pulposus replacement. Biomaterials 2016, 88, 110-9.

Appendix & Supporting Information

Appendix 1: Hydrolytic Degradation Study of varying amounts of SNP-FITC entrapped in UV-PO_{50} with Acid and Base Solutions

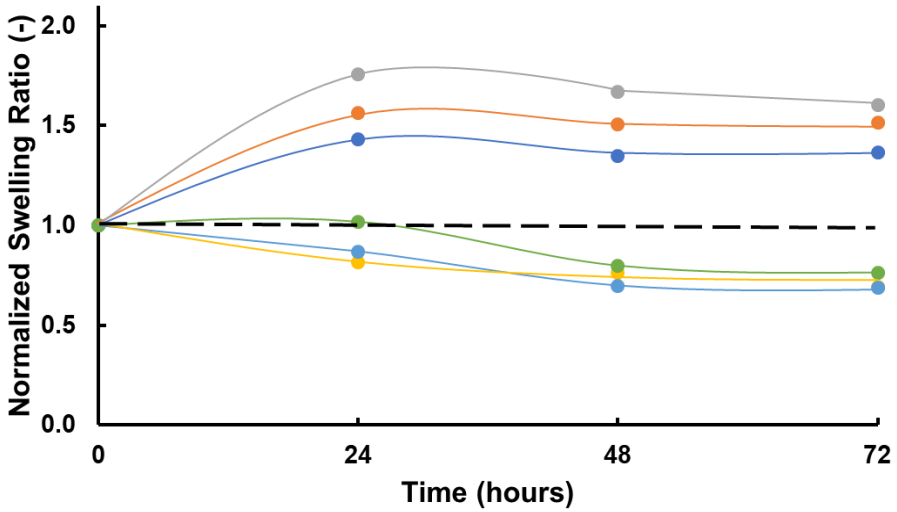

Appendix Figure 2. *Normalized swelling ratio of UV-PO_{50} swollen in different basic solutions. UV-PO_{50}-0.0%wt SNP-FITC swollen in 0.1 M NaOH (●). UV-PO_{50}-1.0%wt SNP-FITC swollen in 0.1 M NaOH (●). UV-PO_{50}-10.0%wt SNP-FITC swollen in 0.1 M NaOH (●). UV-PO_{50}-0.0%wt SNP-FITC swollen in 1.0 M NaOH (●). UV-PO_{50}-1.0%wt SNP-FITC swollen in 1.0 M NaOH (●). UV-PO_{50}-10.0%wt SNP-FITC swollen in 1.0 M NaOH (●). Lines are to guide the eye.*

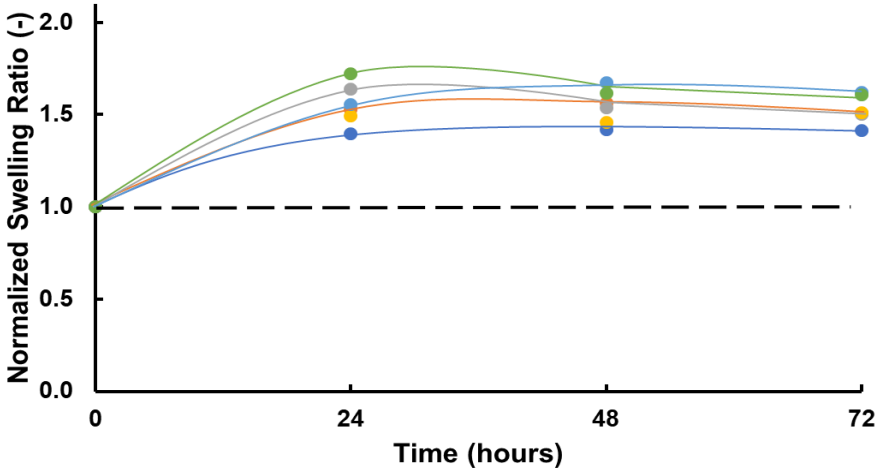

Appendix Figure 1. *Normalized swelling ratio of UV-PO_{50} swollen in different acidic solutions. UV-PO_{50}-0.0%wt SNP-FITC swollen in 0.1 M HCl (●). UV-PO_{50}-1.0%wt SNP-FITC swollen in 0.1 M HCl (●). UV-PO_{50}-10.0%wt SNP-FITC swollen in 0.1 M HCl (●). UV-PO_{50}-0.0%wt SNP-FITC swollen in 1.0 M HCl (●). UV-PO_{50}-1.0%wt SNP-FITC swollen in 1.0 M HCl (●). UV-PO_{50}-10.0%wt SNP-FITC swollen in 1.0 M HCl (●). Lines are to guide the eye.*

Appendix 2: Conductometric Titration of Hydrolytic Degradation of UV-PO_{50}

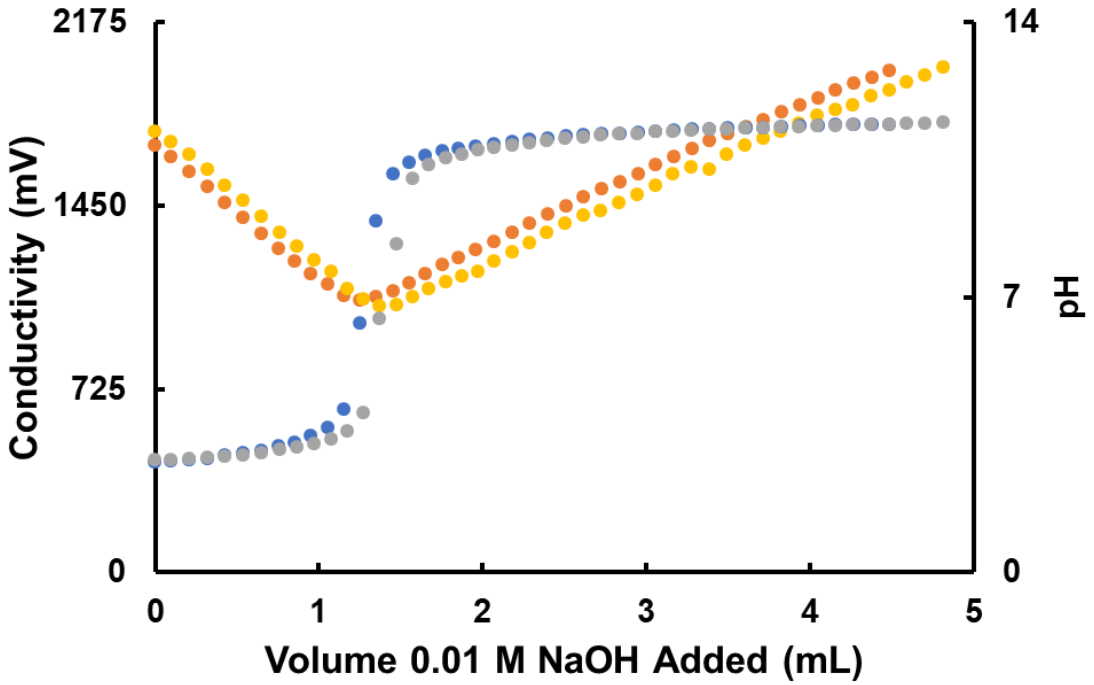

Appendix Figure 3. *Base into acid slow conductometric titration on undegraded (conductivity ● and pH ●) and degraded (conductivity ● and pH ●) UV-PO_{50}-1.0%wt SNP in 20% TFA for 3 hours.*